hclassified

urity classification of this page

REPORT DOCUMENTATION PAGE

a Report Security Classification Unclassified		1b Restrictive Markings	
a Security Classification Authority		3 Distribution Availability of Report	
b Declassification Downgrading Schedule		Approved for public release; distribution is unlimited.	
Performing Organization Report Number(s)		5 Monitoring Organization Report Number(s)	
a Name of Performing Organization Naval Postgraduate School	6b Office Symbol *(if applicable)* 35	7a Name of Monitoring Organization Naval Postgraduate School	
c Address *(city, state, and ZIP code)* Monterey, CA 93943-5000		7b Address *(city, state, and ZIP code)* Monterey, CA 93943-5000	
a Name of Funding Sponsoring Organization	8b Office Symbol *(if applicable)*	9 Procurement Instrument Identification Number	
c Address *(city, state, and ZIP code)*		10 Source of Funding Numbers	
		Program Element No	Project No / Task No / Work Unit Accession No

1 Title *(Include security classification)* IMPROVED AEROSOL OPTICAL DEPTH AND PARTICLE SIZE INDEX FROM SATELLITE DETECTED RADIANCE

2 Personal Author(s) Brian Herbert Miller

3a Type of Report	13b Time Covered From To	14 Date of Report *(year, month, day)*	15 Page Count
Master's Thesis		December 1991	58

6 Supplementary Notation The views expressed in this thesis are those of the author and do not reflect the official policy or position of the Department of Defense or the U.S. Government.

7 Cosati Codes			18 Subject Terms *(continue on reverse if necessary and identify by block number)*
ield	Group	Subgroup	Aerosols, optical depth, particle size index, phase function

9 Abstract *(continue on reverse if necessary and identify by block number)*

An algorithm that extracts aerosol optical depth and particle size index from satellite observations of upwelling radiance over clear ocean areas was modified and studied. In order to examine the algorithm's performance on a regional scale, a previously analyzed data set, retrieved by the NOAA-9 AVHRR sensor, was reprocessed. The area of the study was in the central Pacific Ocean during the RITS-88 cruise from 7 April to 5 May 1988. The results were compared to those of the earlier study and used to investigate changes caused by modifications to the algorithm. One significant modification was to account for the absorption of column water vapor in the calculations. In addition, the correlation between aerosol optical depth and the two-term Henyey-Greenstein phase function was investigated by normalizing measured radiance values.

The results compared well with the earlier study and supported the modifications to the algorithm. Based on this study, aerosol optical depth was shown to be correlated to the Henyey-Greenstein phase function. This knowledge helped in formulating improvements to the phase function.

It was concluded that satellite imaging and processing on a regional scale is a useful way to study marine aerosols, that results can be improved by considering the effects of atmospheric water vapor absorption and other modifications to the calculations, and that there is room for improvement to the two-term Henyey-Greenstein phase function.

0 Distribution Availability of Abstract	21 Abstract Security Classification	
☒ unclassified unlimited ☐ same as report ☐ DTIC users	Unclassified	
2a Name of Responsible Individual Philip A. Durkee	22b Telephone *(include Area code)* (408) 646-3465	22c Office Symbol 63De

D FORM 1473,84 MAR 83 APR edition may be used until exhausted
All other editions are obsolete

security classification of this page

Unclassified

Approved for public release; distribution is unlimited.

Improved Aerosol Optical Depth and Particle
Size Index from Satellite Detected Radiance

by

Brian Herbert Miller
Lieutenant, United States Navy
B.S., University of Wisconsin - Stevens Point, 1980

Submitted in partial fulfillment of the
requirements for the degree of

MASTER OF SCIENCE IN METEOROLOGY
AND PHYSICAL OCEANOGRAPHY

from the

NAVAL POSTGRADUATE SCHOOL
December 1991

Robert L. Haney, Chairman,
Department of Meteorology

ABSTRACT

An algorithm that extracts aerosol optical depth and particle size index from satellite observations of upwelling radiance over clear ocean areas was modified and studied. In order to examine the algorithm's performance on a regional scale, a previously analyzed data set, retrieved by the NOAA-9 AVHRR sensor, was reprocessed. The area of the study was in the central Pacific Ocean during the RITS-88 cruise from 7 April to 5 May 1988. The results were compared to those of the earlier study and used to investigate changes caused by modifications to the algorithm. One significant modification was to account for the absorption of column water vapor in the calculations. In addition, the correlation between aerosol optical depth and the two-term Henyey-Greenstein phase function was investigated by normalizing measured radiance values.

The results compared well with the earlier study and supported the modifications to the algorithm. Based on this study, aerosol optical depth was shown to be correlated to the Henyey-Greenstein phase function. This knowledge helped in formulating improvements to the phase function.

It was concluded that satellite imaging and processing on a regional scale is a useful way to study marine aerosols, that results can be improved by considering the effects of atmospheric water vapor absorption and other modifications to the calculations, and that there is room for improvement to the two-term Henyey-Greenstein phase function.

TABLE OF CONTENTS

LIST OF TABLES

LIST OF FIGURES

ACKNOWLEDGMENTS

I thank Professor Philip A. Durkee for his assistance, guidance, and understanding support during the course of my research. His interest in and insight into the field of satellite meteorology inspired me to seek him out as an advisor and mentor. I am grateful for having had the opportunity to work with him. I also thank Professor Carlyle H. Wash for his careful review of my thesis as well as for his helpful suggestions for improvement. I commend the staff of the Naval Postgraduate School's Interactive Digital Environmental Analysis (IDEA) laboratory for their support. I especially thank Mr. Craig E. Motell, whose patience and determination in programming and data interpretation saved me many hours of additional work. Indeed, I would have been hard pressed to finish this thesis on time without Mr. Motell's help. I thank my parents, Herbert P. Miller and Gisela H. Miller, for their continued interest in my work and lastly, I thank my wife, Argelia, for her unwavering love and faith in me during the many hours I spent away from her while completing this thesis.

I. INTRODUCTION

A. THE NATURE OF THE PROBLEM AND BACKGROUND

As the world's population and knowledge have grown, so too has an interest in its climate. The ability to study our environment and anticipate possible climate changes, whether caused by humans or not, has far-reaching implications for future generations. Their very survival may depend not only on our ability to understand any changes, but also on what we do about them, whether it be to adapt to the changes or attempt to influence our climate. How well we might adapt to changes or whether we can influence our climate is still not known but we have begun to understand it by studying the overall radiation budget of the earth.

Prior to the advent of the satellite, estimates of radiation entering and leaving the earth-atmosphere system were made using radiative transfer equations (Rao et al. 1990). Many factors had to be considered and incorporated into the model. Radiation in the atmosphere is attenuated by many processes. It is absorbed and scattered by molecules of air, aerosols, and meteorological features such as clouds, precipitation and fog. Aerosols are solid and liquid particles, approximately one micron or less in diameter, suspended in air. This includes smoke, dust, haze, and some clouds. While the results of the radiation calculations were helpful, there are still many uncertainties. For example, in recent years there has been increasing interest in the warming of the earth's climate caused by increased concentrations of the so-called greenhouse gases, notably CO_2 , which trap outgoing long wave radiation.

It was and still is necessary to parameterize the less well understood contributions of such features as aerosols and clouds. These features are inherently more difficult to measure than CO_2 because they have shorter time scales and they arise on a local or regional scale leading to higher variability. Sources of aerosols include natural, like volcanic aerosols and desert dust, anthropogenic, or human made, and biological, where gaseous metabolic byproducts are precursors to aerosols. McCormick and Ludwig (1967) proposed that a buildup of aerosols could have a cooling effect on the earth. Charlson and Pilat (1969) concluded that particle size distribution as well as scattering and absorption cross sections also played a role and could lead to warming in some cases, especially for anthropogenic aerosols. Coakley et al. (1983) studied naturally occurring tropospheric aerosols and found that they result in global surface cooling of 2-3

°C, an amount close to the increase in temperature due to such gases as CH_4 and N_2O, or a doubling of CO_2. In addition, the cooling effect of aerosols can be multiplied when they act as cloud condensation nuclei (CCN) resulting in the formation of cloud droplets. Clouds reflect incoming solar radiation leading to a cooling effect. Opposing this effect is a tendency for non-nucleated anthropogenic aerosols to absorb radiation thereby reducing cloud reflectance which leads to warming. Twomey (1977) and Twomey et al. (1984) concluded that for thin and medium optically thick clouds over continents, an increase in anthropogenic aerosols results in cooling. Thin and medium optically thick clouds are most common in the atmosphere. Thus, fluctuations in aerosol concentration could play a role in the global climate with an increase in aerosol concentration contributing to a cooling effect.

Furthermore, Charlson et al. (1987) has expanded on hypotheses of Shaw (1983) and later Lovelock (1986) that a biological feedback mechanism where marine phytoplankton, through production of marine aerosol precursors, play a role in climate regulation.

Figure 1 is a schematic diagram of how the feedback mechanism works. In the diagram the rectangles are measurable quantities and the ovals are processes linking the rectangles. A positive sign in the oval indicates the effect a positive change in the previous rectangle has on the following rectangle. A negative sign has a negative effect on the following rectangle for a positive change in the previous rectangle.

Charlson et al. (1987) explain that the dimethylsulfide (DMS) produced by phytoplankton is oxidized in the atmosphere to form a non-sea-salt sulfate ($NSS\text{-}SO_4^{2-}$). These $NSS\text{-}SO_4^{2-}$'s act as CCN in the marine atmosphere. The argument is that DMS is produced in sufficient quantity to be the primary source of CCN in the remote, unpolluted marine atmosphere. Since clouds form from CCN, and clouds act to reflect incoming solar radiation, phytoplankton might then play a role in regulating the earth's climate. The greatest uncertainty in the hypothesis is what effect any lowering of the earth's surface temperature and reduction of solar irradiance below the clouds would have on the phytoplankton and DMS production.

Once satellites became available they were quickly tasked to help provide data on radiation or factors that influence radiation (Rao et al. 1990). For example, marine aerosols are atmospheric constituents that appear to play an important role in the overall radiation budget, as was shown. Hindman et al. (1984) describe experiments that establish a positive relationship between aerosol variations and satellite detected brightness variations in the marine boundary layer. In fact, direct measurements of marine

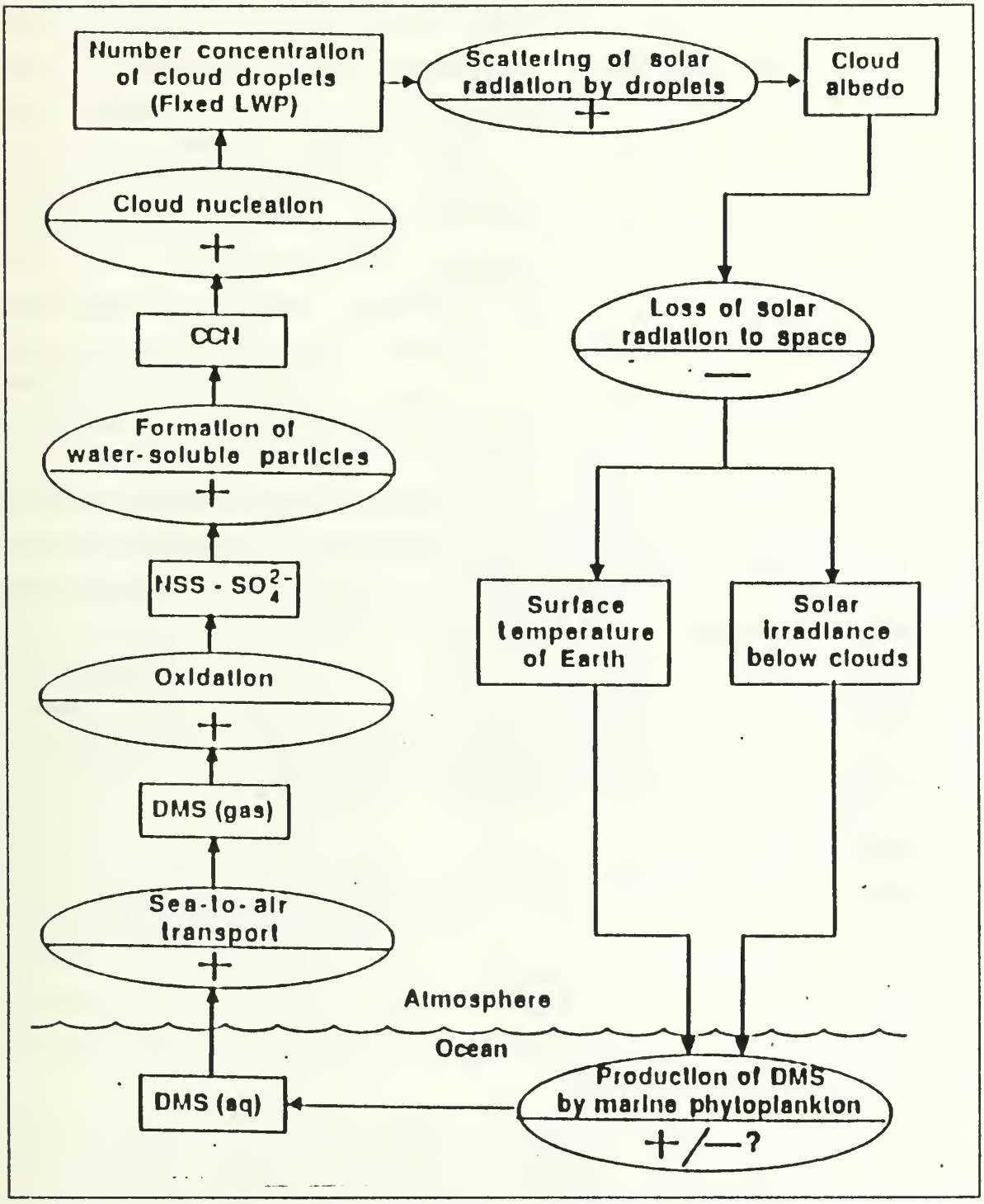

Figure 1. Biological feedback in the Earth's radiation budget (Charlson et al. 1987): rectangles are measured quantities, ovals are linking processes. Plus or minus signs indicate the effect a positive change in a previous rectangle has on the following rectangle.

aerosol characteristics could be provided by ship or aircraft. While this information is valuable, it is expensive and difficult to obtain and only a small area of the world's oceans can be sampled and studied at a time. Satellites, on the other hand, can provide near continuous data over large areas. This capability is desirable for evaluating the effects of aerosols on a global scale. Meteorological satellites, however, have been designed to measure cloud albedo while sensitivities to radiances associated with aerosol optical depth variations are small (Durkee 1984). Thus, in order to determine aerosol characteristics, it is important that the satellite data be carefully processed.

Aerosols can also play a role in military applications. Aerosols can scatter energy from a laser beam propagating through the atmosphere. Lasers can be used for satellite communications with submarines. The narrow beam of the laser is harder to detect than the normal radio communications now in use and is capable of higher data transmission rates to deeper depths. As submarines become more important as multimission platforms, it becomes more important to have secure communications with them (Painter 1989). In addition, line-of-sight communications operating in the near infrared can utilize aerosol scatter in the marine boundary layer to provide over-the-horizon ranges of 30-300 miles (Mooradian 1981).

Further investigations of aerosol characteristics are clearly needed. The purpose of this thesis is to better utilize satellite data in order to more accurately measure aerosol characteristics so that their effect on the overall radiation budget of the earth and in other applications such as communications may be quantified.

B. METHODOLOGY

Durkee et al. (1991) describes an algorithm whereby multispectral radiance data obtained from the Advanced Very High Resolution Radiometer (AVHRR) onboard the U.S. National Oceanic and Atmospheric Administration (NOAA)-9 satellite is used to obtain estimates of aerosol optical depth and particle size index over clear ocean areas. By utilizing different satellite channel sensitivities, the particle size index can be measured and the optical depth calculated.

Modifications to the algorithm have been made. For example, Mahony (1991) studied and quantified the effects of column water vapor absorption on aerosol particle size index. This information can be used to improve the performance of the algorithm. In addition, a modification to account for variable earth-sun distance on solar irradiance was made. A change in the computer code to correct a mathematical error and an adjustment to an over correction for ozone absorption were the final two modifications.

To study the modified algorithm on a regional scale, a data set used by Benedict (1989) was reprocessed. The results were compared to those of Benedict's (1989) earlier study. It was expected that all the modifications would improve the results with the water vapor correction being the most significant. An important extension of this procedure was to study the correlation between optical depth and the two-term Henyey-Greenstein (HG) phase function used in the calculations. This was accomplished by studying a plot of normalized measured radiance versus scattering angle for various particle size indices. The purpose of doing this was to make optical depth independent of scattering angle; these variables might be related through the phase function. If there is a correlation, improvements to the phase function and therefore calculated optical depth are indicated.

This methodology was chosen because the Benedict (1989) data set was available and provided a baseline from which to measure improvements. In addition, useful information about the HG phase function had not yet been extracted from the Benedict (1989) data set. Once improvements to the algorithm are verified and permanently incorporated into the computer code, new data sets can be studied with the goal of better understanding the role of DMS on the earth's climate.

C. OBJECTIVES

The specific objectives of this thesis are to compare the results to those of Benedict's (1989) study and note changes caused by modifications to the algorithm. In addition, improvements to the results derived from Mahony's (1991) correction for atmospheric water absorption will be studied. Finally, the form of the Henyey-Greenstein phase function obtained from this study is compared to that used by Frost (1988) in order to make recommendations for improvement.

II. THEORY

A. RADIATIVE TRANSFER

It will be shown in the following discussion that satellite measurements of upwelling radiance provide a means to determine aerosol optical depth and particle size information. These characteristics can help determine the amount and source of aerosols. The satellite wavelengths used in the approach are from the NOAA-9 AVHRR. Table 1 gives channel bandwidths for reference.

Table 1. AVHRR CHANNEL BANDWIDTH: (in microns) from Kidwell (1986).

Channel	Radiance	Bandwidth
1	Visible	0.58 - 0.68
2	Red/Near Infrared	0.70 - 1.10
3	Thermal Infrared	3.50 - 3.90
4	Thermal Infrared	10.30 - 11.50
5	Thermal Infrared	11.30 - 12.40

In order to develop a practical form of the Radiative Transfer Equation (RTE) for use in marine aerosol calculations, it is necessary to review the theory and make some assumptions and modifications. From Liou (1980), the form of the RTE in a plane parallel atmosphere for scattering radiation is

$$\mu \frac{dL(\delta, \Omega)}{d\delta} = L(\delta, \Omega) - \frac{\omega_o}{4\pi} \int_0^{4\pi} L(\delta, \Omega') p(\Omega, \Omega') d\Omega'$$

$$- \frac{\omega_o}{4\pi} \pi F_o p(\Omega - \Omega_o) e^{-\delta/\mu_o},$$

where

L = Diffuse intensity of radiance.

δ = Optical depth.

ω_o = Single scattering albedo.

μ = cos θ (observation zenith angle).

μ_o = cos θ_o (solar zenith angle).

Ω = Solid angle (θ, ϕ) (ϕ = azimuth angle).

Ω_o = Solid angle of direct radiation singly scattered into the path.

Ω' = Solid angle of multiply scattered radiation scattered into the path.

$p(\Omega, \Omega')$ = Scattering phase function from solid angle Ω to Ω' (Θ).

πF_o = Incoming radiative flux (solar flux density) adjusted for variable earth-sun distance; different for channels one and two.

The first term on the right represents the diffuse radiance attenuated from the beam by single scatter and absorption while the second and third terms represent contributions from multiple and single scatter into the beam, respectively.

Optical depth is defined as the amount of absorbing material lying between two levels and can be represented as

$$\delta = \int_0^H \sigma_{ext}\, dz, \tag{2.1}$$

where σ_{ext} is the extinction coefficient and H is the satellite height. The extinction coefficient, which is a sum of absorption and scattering contributions, is defined as

$$\sigma_{ext} = \int_0^\infty \pi r^2\, Q(m, \lambda, r)\, \frac{dN(r)}{dr}\, dr, \tag{2.2}$$

where πr^2 is the particle cross sectional area, Q(m, λ, r) is the extinction efficiency for either scattering or absorption as a function of the complex index of refraction, the wavelength, and the particle radius, and $dN(r)/dr$ is the slope of the aerosol size distribution.

For marine particles absorption is negligible when the wavelength is less than one micron. Then σ_{ext}, which equals the sum of the extinction from scattering and absorption, is nearly equal to σ_{scat} (Shettle and Fenn 1979). The single scattering albedo is defined as σ_{scat} divided by σ_{ext} and is nearly equal to one.

The scattering phase function, $p(\Theta)$, is the distribution of scattering by particles and is equal to one when summed over all solid angles. More will be said about the phase function below.

If multiple scattering is neglected and only single scattering of direct solar radiation into the path is assumed, the RTE simplifies to (Liou 1980)

$$L(\delta;\mu,\phi) = L(\delta_1;\mu,\phi)\exp[-(\delta_1-\delta)/\mu] +$$

$$\pi\frac{\omega_o}{4\pi}F_o p(\mu,\phi;-\mu_o,\phi_o)\int_{\delta}^{\delta_1}\exp\{-[(\delta'-\delta)/\mu+\delta'/\mu_o]\}\ d\delta'/\mu,$$

where δ_1 is the optical depth at the bottom of the atmosphere and δ' is the increment of optical depth between the bottom of the atmosphere and the level of interest.

Additionally, over ocean areas in the red and near infrared wavebands there is very little radiation emitted by the earth resulting in a further simplification of the RTE at the top of the atmosphere to (Liou 1980)

$$L(0;\mu,\phi) = \frac{\omega_o\mu_o F_o}{4(\mu+\mu_o)}p(\Theta)\{1-\exp[-\delta_1(1/\mu+1/\mu_o)]\}. \tag{2.3}$$

For optically thin atmospheres, where optical depth is less than about 0.1, which is true over clear ocean areas, $\delta_1(1/\mu + 1/\mu_o) \ll 1$ and equation 2.3 reduces to (Durkee 1984)

$$L(0;\mu,\phi) \approx \frac{\omega_o F_o}{4\mu}p(\Theta)\delta_1. \tag{2.4}$$

Now the upwelling radiance can be broken down into its various contributions as

$$L_{Total} = L_{Molecules} + L_{Aerosols} + L_{Sunglint} - L_{Ozone},$$

where the subscripts stand for the contributions by molecules, or Rayleigh scatter, contributions from aerosols, contributions from sun glint, or specular reflection, and reduction by ozone absorption, respectively.

To get the aerosol radiance, the radiance measured by the satellite sensor was adjusted by subtracting the Rayleigh scatter due to molecules following Turner (1973). Rayleigh scatter occurs when the size of the particle is much smaller than the wavelength of incident radiation and though strongly wavelength dependent, it does not vary spatially.

An adjustment for sun glint is also necessary. Ramsey (1968) showed that sea surface reflectance is very small for red wavelengths (albedo = 0.5%) and zero for radiation with wavelengths greater than 0.7 microns, except where the sun-earth-satellite geometry results in sun glint. Therefore, geometries which could contribute to sun glint are avoided. Following Cox and Munk (1954), an angle of reflection is calculated from ge-

ometry considerations. Then an elliptical area in the neighborhood of the reflection point where sun glint is possible is defined. This definition is based on the angular diameter of the sun.

Since ozone absorbs weakly in channels one and two, a small ozone correction was added back. This correction was a modification to that of Benedict (1989). Now the aerosol radiance, L_A, can be expressed as

$$L_A = L(0; \mu, \phi) - L_M - L_{SG} + L_O \approx \frac{\omega_o F_o}{4\mu} p(\Theta)\delta_A, \tag{2.5}$$

where δ_A is aerosol optical depth.

Griggs (1975) and Durkee et al. (1986) showed that there is indeed a linear relationship between aerosol radiance and optical depth. A method is now available to obtain aerosol optical depth from upwelling radiance by rearranging equation 2.5 to give

$$\delta_A = \frac{L_A 4\mu}{\omega_o F_o p(\Theta)}. \tag{2.6}$$

By taking the ratio of channel one to channel two aerosol radiance, given by

$$\frac{L_{Red}}{L_{NIR}} \sim \frac{(\omega_o F_o/4\mu)p(\Theta)(\delta_{Red})}{(\omega_o F_o/4\mu)p(\Theta)(\delta_{NIR})},$$

a new parameter, the particle size index, is defined from which particle size information can be obtained:

$$S_{12} = \frac{L_{Red}}{L_{NIR}} \approx \frac{\delta_{Red}}{\delta_{NIR}}. \tag{2.7}$$

Since for smaller particles the aerosol dependent terms, ω_o, $p(\Theta)$, and δ are larger at red wavelengths (Durkee 1984), smaller particles would cause S_{12} to be larger. The increase in optical depth can be attributed to a steeper slope in the particle size distribution as seen from equations 2.1 and 2.2. Thus the particle size index gives an indirect measure of the aerosol particle size distribution. For channels one and two the radiances are such that S_{12} is normally greater than one.

B. THE HENYEY-GREENSTEIN VARIABLE PHASE FUNCTION

The scattering phase function describes the fraction of radiation scattered in a given direction. As discussed by Frost (1988), one single phase function is inadequate for

calculating optical depth when aerosols change over global scale areas. Therefore, a variable phase function, the two-term Henyey-Greenstein phase function (Lenoble 1985), was chosen and is given by

$$p(\Theta) = \frac{\alpha(1-g_1^2)}{(1+g_1^2-2g_1\cos(\theta))} + \frac{(1-\alpha)(1-g_2^2)}{(1+g_2^2+2g_2\cos(\theta))}, \tag{2.8}$$

where α is a weighting factor and g_1 and g_2 are asymmetry curve factors. All are empirical functions of S_{12} (Frost 1988) and are given by

$$\alpha = 1.2 - (0.25 \times S_{12}),$$

$$g_1 = 1.04 - (0.08333 \times S_{12}),$$

and

$$g_2 = 1.2 - (0.58333 \times S_{12}).$$

Figure 2 shows a plot of the phase function versus scattering angle for various S_{12} values. Higher values of the particle size index (smaller particles) result in a curve that is closer to that of Rayleigh scattering. The HG phase function uses S_{12} prior to correction for Rayleigh scattering and ozone absorption. Since Rayleigh scattering, more in channel one, increases S_{12} and ozone absorption, also more in channel one, decreases S_{12}, the difference is slight and the resulting particle size index and phase function do not vary greatly from corrected values (Durkee et al. 1991).

The HG phase function also varies with wavelength although it is only shown here for channel one. This introduces an error into the calculation of optical depth for channel two in equation 2.6. It will be shown in the analysis of results how this error may be corrected.

C. WATER VAPOR CORRECTION TO THE PARTICLE SIZE INDEX

The RTE in the above calculations assumed cloud free conditions. Another important consideration in atmospheric absorption is the moisture present in the atmosphere. Water vapor can produce as much as a 15% error in the phase function and aerosol particle optical depth (Mahony 1991). Dalu (1986) developed an algorithm to measure water vapor content using the channel four and five brightness temperature difference. The measured water vapor content of a column of air is used to determine the "dry" aerosol particle size index.

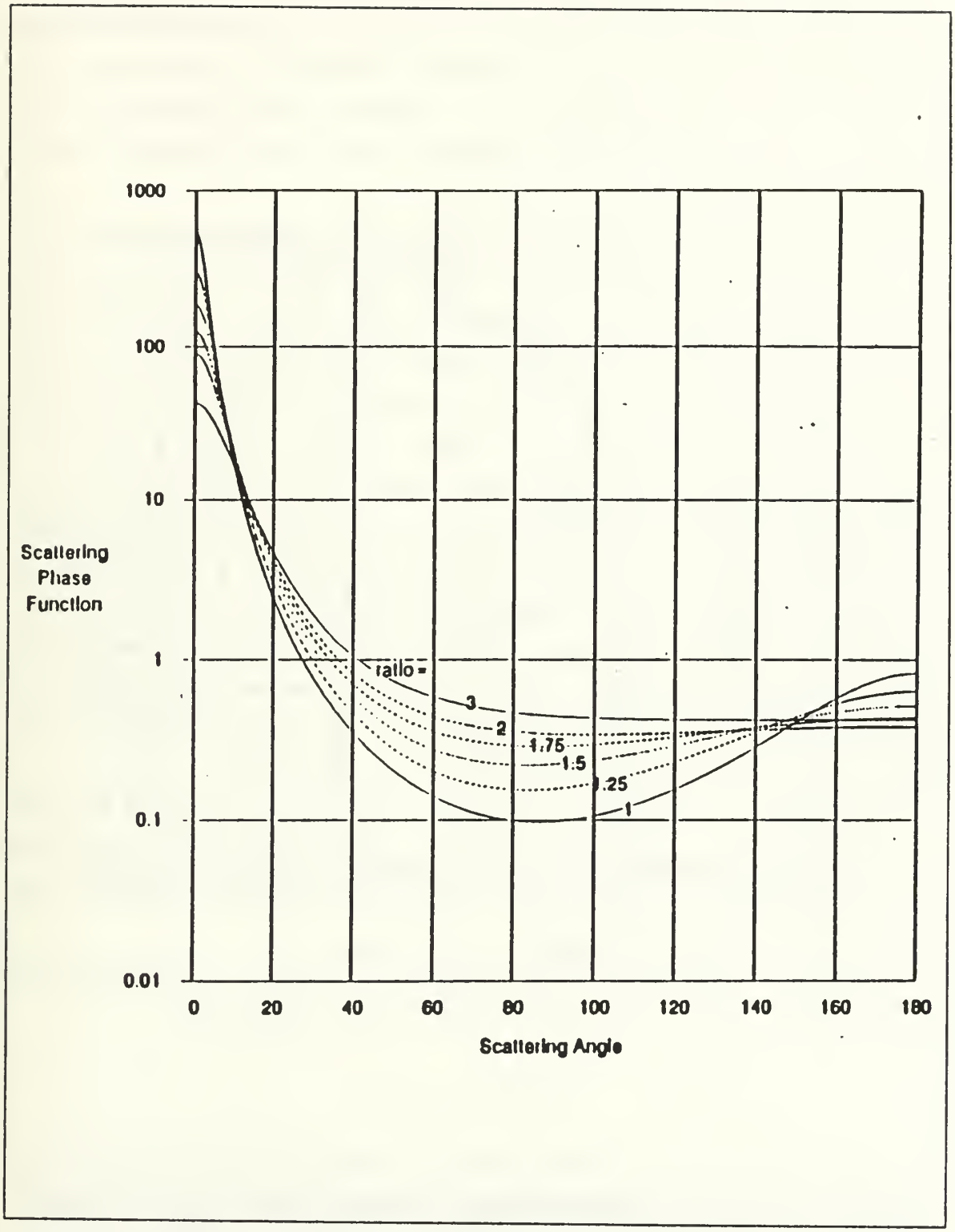

Figure 2. The Henyey-Greenstein (HG) scattering phase function (Frost 1988)

In Figure 3 the effect of water vapor can be seen in the transmittance (τ) for AVHRR channels one and two. Note that for channel one τ is greater than channel two indicating less absorption. Channel two radiance would tend to decrease more than channel one leading to overestimation of S_{12}. This error could be misinterpreted as a change in aerosol properties or it could mask real changes. Thus, accounting for water vapor should improve the accuracy of the results.

Mahony (1991) used the U.S. Air Force's Low Resolution Transmittance (LOWTRAN)-7 atmospheric propagation model to study the effects of water vapor. Figure 4 shows the channel one and two relative response as well as the resulting radiances from Rayleigh scatter, Rayleigh and aerosol scatter, and Rayleigh plus aerosol scatter minus water vapor absorption. The radiances increase with smaller wavelength as the contribution from Rayleigh scatter increases. The radiance decreases with wavelength in both channels but more in channel two leading to overestimation of S_{12}.

An estimate of the water vapor content in an air column can be made using channels four and five of the AVHRR, at 11 and 12 microns respectively. Here absorption by water vapor is dominant while scattering is relatively insignificant. The benefits of using these channels are their collocation and temporal linkage with channels one and two, providing a water vapor snapshot along the same path as aerosol optical depth measurements. Although not the ideal sensor window for water vapor content, their use is justified within the accuracy of the approximations (Mahony 1991).

The brightness temperature (T) is determined from the radiance received due to direct transfer from the ocean surface to the satellite sensor. Therefore the transmittance is directly proportional to the retrieved T. Only absorption reduces the radiance reaching the sensor, scattering is negligible.

Dalu (1986) showed that by using the difference in brightness temperature between channels four and five the water vapor content could be obtained from

$$w = A(T_4 - T_5)\cos\theta,$$

where w is the water vapor content in grams per square meter and T_4 and T_5 are the brightness temperatures in degrees Kelvin for channels four and five, respectively, and θ is the scanning angle. The constant A is equal to 19600 grams per degree Kelvin per meter squared.

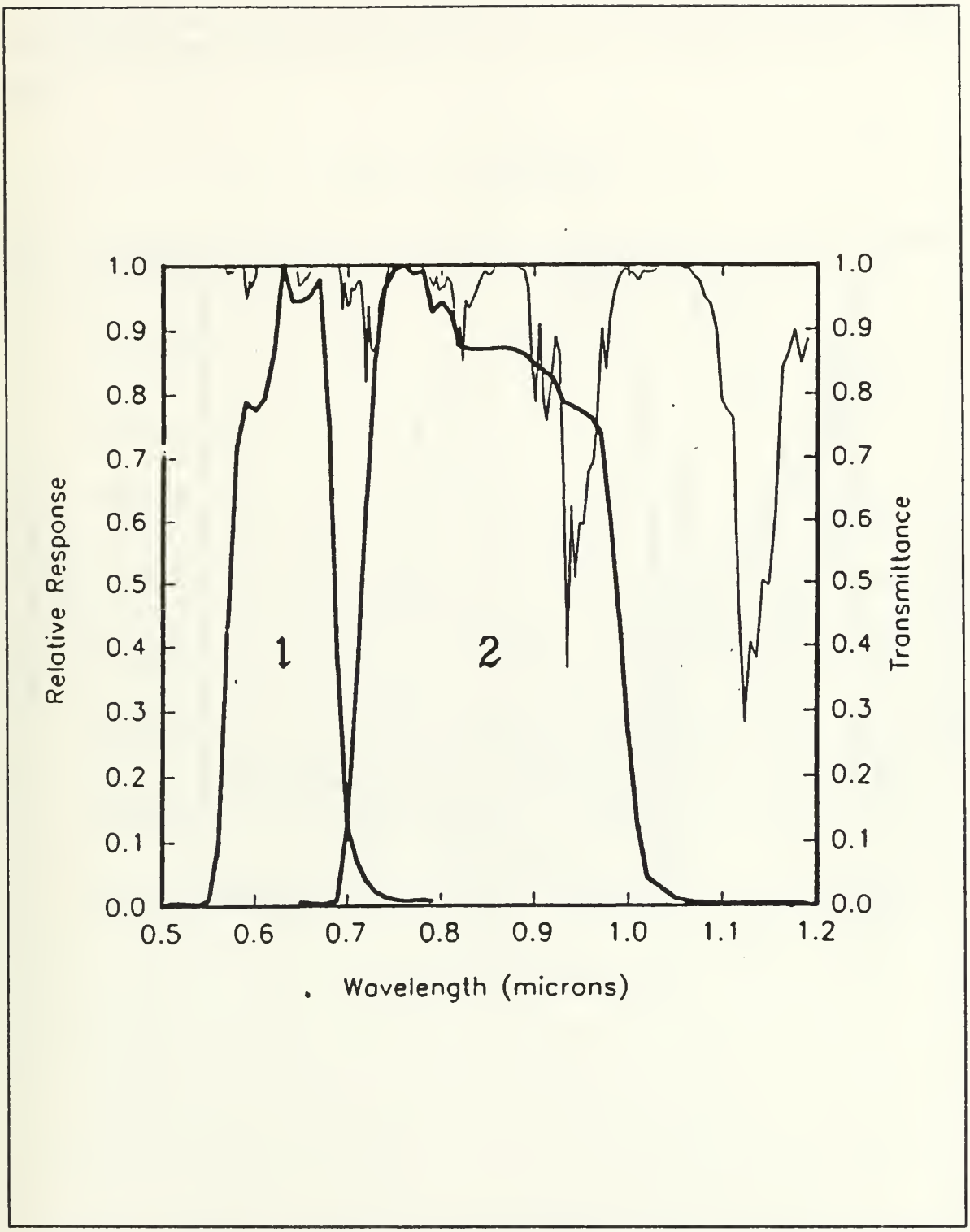

Figure 3. Water vapor effects on NOAA-7 channels one and two (Mahony 1991): total transmittance is superimposed.

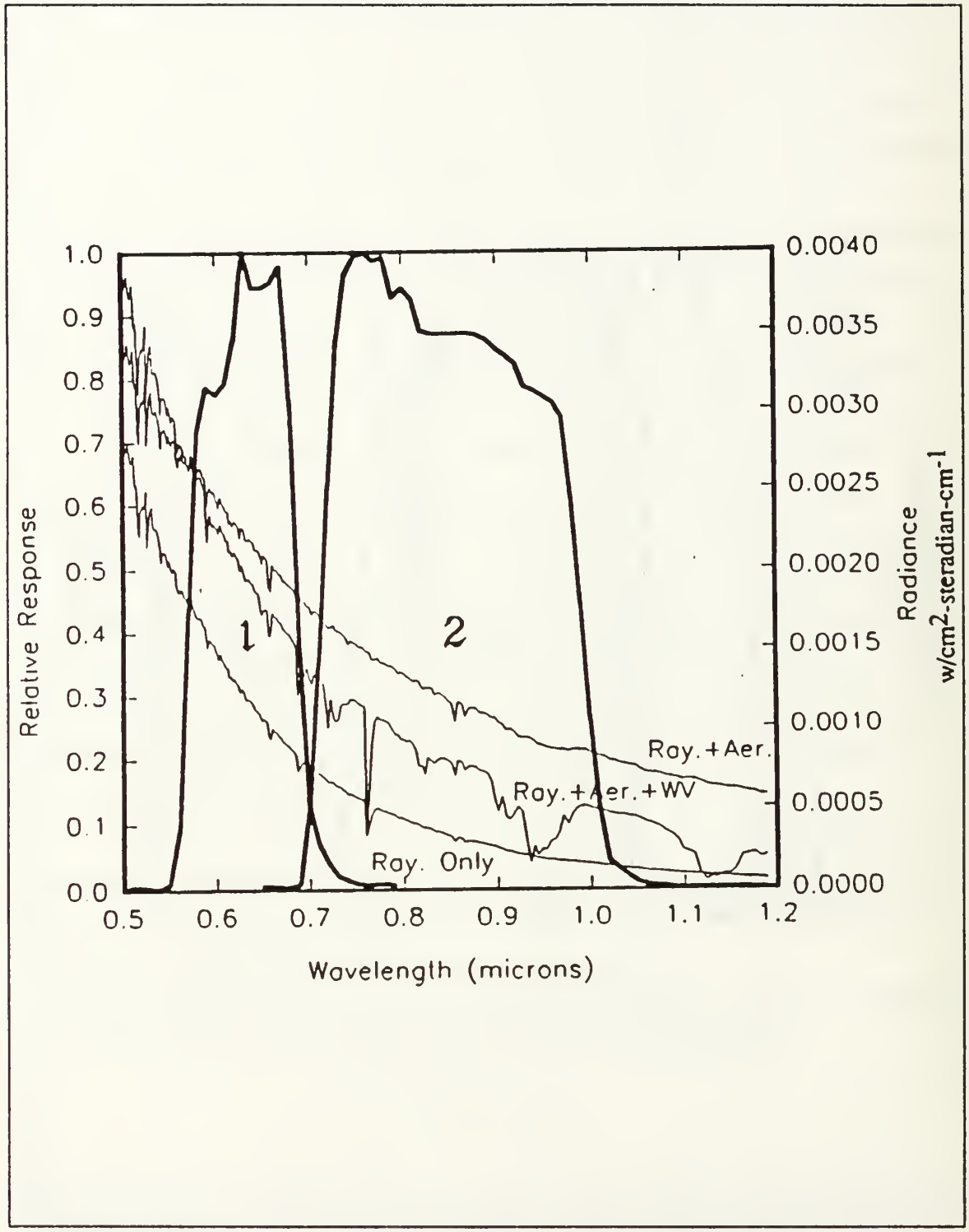

Figure 4. **Water vapor influence on atmospheric radiation (Mahony 1991):** NOAA-7 response curves and LOWTRAN-7 used.

By comparing the water vapor content to the particle size index, Mahony (1991) obtained the following empirical relation for the particle size index corrected for water vapor:

$$S_{12}(\text{dry}) = \frac{S_{12}}{(1 + .0332\sqrt{w})},$$

where w is the water vapor content in grams per square centimeter. This is the formula used in the calculations to obtain dry optical depth and particle size index.

III. PROCEDURE

A. THE DATA SET AND THE SATELLITE

The in-situ measurements were taken from the *Research Vessel (R/V) Oceanographer*, a NOAA funded research vessel, during the Radiatively Important Trace Species (RITS)-88 cruise conducted from 7 April to 5 May 1988. The ship's track was in the central North and South Pacific Oceans from 50°N to 12°S along 170°W. Data measurements were obtained for every one degree of latitude and included DMS emissions in the sea and air, NSS-SO_4^{2-} aerosol concentration, aerosol size distribution, and total particle concentration (Charlson and Bates 1989). Optical depth was also obtained using a hand held photometer.

The satellite data were collected by the AVHRR sensor onboard the NOAA-9 satellite. See Table 1 for AVHRR channel wavelength bands. The NOAA-9 is a sun-synchronous, near polar-orbiting satellite with local equator crossing times of 0220, descending, and 1420, ascending. It has a nominal altitude of 833 km and resolution of 1.1 x 1.1 km at sub-point.

The satellite data utilized were for the same time frame and area as the ship's track from the digital archives of the National Environmental Satellite and Information Service (NESDIS). The 57 passes were stored as Global Area Coverage (GAC) data; GAC is an archiving technique that also reduces the resolution at sub-point to about 4.0 x 4.0 km.

B. PROCESSING FACILITIES

The data were processed at the Interactive Digital Environmental (IDEA) Laboratory at the Naval Postgraduate School in Monterey, California. The main computer was a Digital Equipment Corporation VAX 8250 with graphics display terminals. Processing included loading and reading the magnetic tapes to memory and then processing the data. The multi-channel analysis routine used to analyze the data was a FORTRAN program run on the VAX computer. Visual images were also produced in the IDEA lab and helped in the interpretation and analysis of the data.

C. THE ALGORITHM

The satellite data were analyzed using a scheme developed by Pfeil (1986) and modified by Frost (1988). In addition, corrections were made to solar irradiance to ac-

count for variations in earth-sun distance, for over correction of ozone absorption, and to correct the computer code for a mathematical error. Calculations were also made using the water vapor correction to S_{12} described by Mahony (1991).

The pixels were subjected to a number of filters, described below, and composited in one degree by one degree boxes. To study the relationship between satellite and shipboard measurements, channel one aerosol optical depth and the particle size index were further filtered geographically to within five degrees longitude of 170° W and plus or minus three days of the ship's track.

The first step in the algorithm is to test for valid data. After reading in the data and determining their geographical position, only data equatorward of 70°N or S is accepted. In addition, the data are required to be over ocean areas; here upwelling radiance from the surface is minimized. Next, sun angle is checked. Solar zenith angle must be less than 70° to avoid longer and more complicated optical paths. Data with specific geometries in relation to the satellite are also eliminated to avoid sun glint (Cox and Munk 1954). This eliminated a large portion of the western half of each pass.

Before testing the pixels further, an adjustment to channels one and two were made to account for ozone absorption. This is of greatest concern for a wavelength of 0.69 microns (Durkee et al. 1991).

The calibrated pixels are then further processed to determine cloud contamination. If the brightness temperature of channel four is less than 273°K, the pixel is assumed to be contaminated by high clouds. Next, if the channel two albedo is greater than 40%, the pixel is assumed to be contaminated by low clouds. Then, if the channel one divided by channel two albedo ratio is greater than 1.5, the pixel is considered clear since cloud scattering is weakly dependent on wavelength. If the ratio is less than 1.5, the pixel undergoes further testing. The channel two albedo is compared to that of the pixels above, below, and to the left and right. If the difference between the maximum and minimum counts is less than five, the pixel is clear, otherwise it is partly cloudy. A count is approximately 0.1069% albedo (Kidwell 1986).

Once a clear pixel has been determined, the Rayleigh radiance is subtracted from channels one and two (Turner 1973) and the optical depth and particle size index are calculated using equations 2.6 and 2.7. The derived parameters are:

The Spatial Variables. Channel one and two radiances were used to obtain optical depth and particle size index. The "dry" values were also obtained using the algorithm of Mahony (1991). This information was composited temporally over the entire data set and was used to create images.

The Geometry Variables. These are variables such as normalized measured radiance as a function of scattering angle, latitude, and particle size index. They were composited geographically across all longitudes as well as temporally. One parameter, the normalized measured radiance as a function of scattering angle for different particle size indices, was used to study the two-term HG phase function.

The Daily Variables. The particle size index and channel one optical depth both uncorrected and corrected for water vapor filtered to be within five degrees of longitude and plus or minus three days of the ship's track. This information was used for comparisons with in-situ measurements.

The calculated values were then stored in data files and used as needed to produce the necessary images and plots for comparison with those of Benedict (1989) and the measurements of the *R/V Oceanographer*.

IV. RESULTS AND DISCUSSION

The results are organized to show improvement to the analysis done by Benedict (1989), to show improvements to aerosol characteristics based on corrections for column water vapor as parameterized by Mahony (1991), and to investigate improvements to the HG variable phase function.

Before looking at the results, it is useful to examine a summary of the synoptic situation during the 7 April - 5 May 1988 time frame. The synoptic situation is important to the discussion since it helps identify sources of aerosol particles. Knowing the sources of the aerosols helps in interpreting the results.

Representative Navy Operational Global Atmospheric Prediction System (NOGAPS) surface pressure and 500mb height patterns are shown in Figures 5 and 6. A generally westerly flow exists over the Asian continent in the 35-45°N latitude band indicating a source for natural and anthropogenic continental aerosols. Natural aerosols would tend to be larger in size than the marine aerosols being studied. Benedict (1989) discusses the occurrence of KOSA, or dust clouds from storms in the Gobi desert during April. Given typical translational rates (Shaw 1980), the dust from these storms could influence the aerosol concentration in the central Pacific.

Another environmental factor discussed by Benedict (1989) was the eruption of the Kilauea volcano in Hawaii (17°N, 157°W) producing a continual source of aerosols during this time frame. These aerosols were initially dominated by gaseous sulfur compounds which later changed to the solid phase in the atmosphere and grew as they migrated downstream. The debris from the eruption was carried across the path of the *R/V Oceanographer's* track by the Northeast Tradewinds and influenced the aerosol measurements.

The composite optical depths for the entire experimental period are shown in Figures 7 and 8. The optical depth is an indication of both the number and size of aerosols. The uncorrected optical depth is presented in Figure 7 which shows an area of relatively low optical depth in its lower right corner. A higher optical depth was expected due to the volcanic aerosols. The reason for the low optical depth is because most of the volcanic emissions are gaseous and very small and therefore do not greatly effect optical depth. It is also possible that the parameterization of the phase function is not correct leading to errors in optical depth. Figure 7 shows an area of high optical depth at the

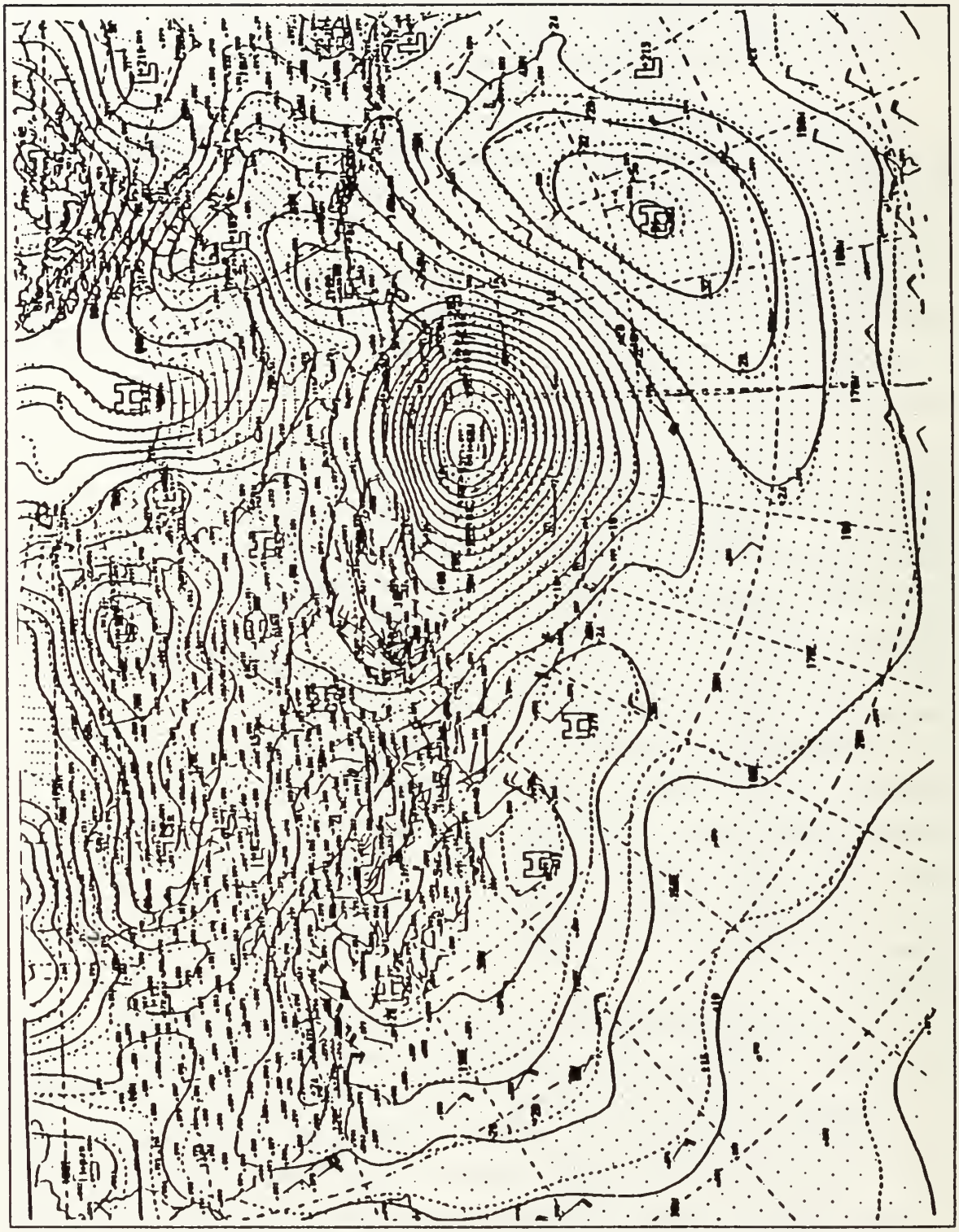

Figure 5. NOGAPS 1200 UTC 10 April 1988 Surface Analysis (Benedict 1989)

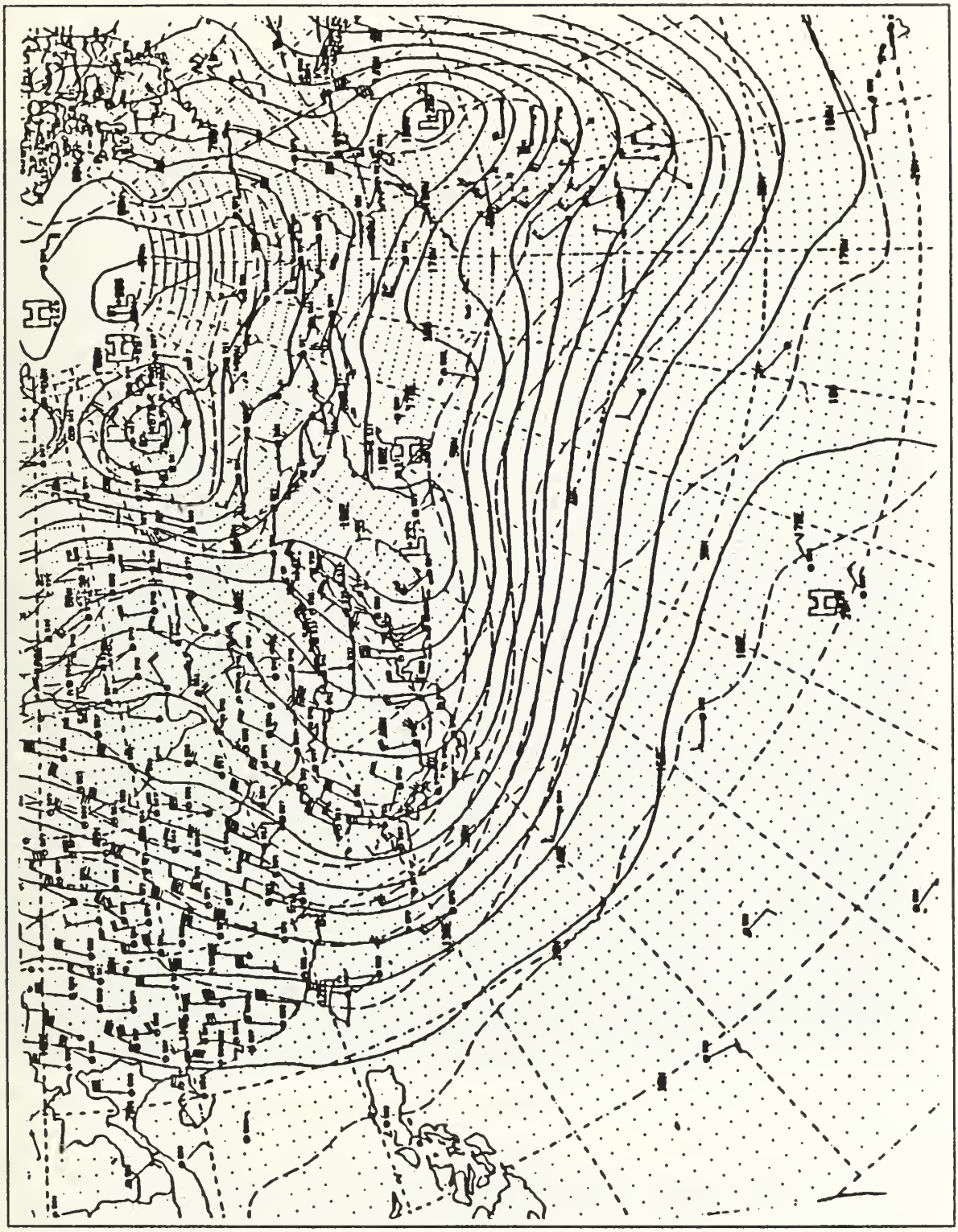

Figure 6. NOGAPS 1200 UTC 10 April 1988 500mb Analysis (Benedict 1989)

western edge of the area which extends eastward across the upper third of the figure. This indicates a potentially large number of particulates which could be either anthropogenic or natural in origin. When the particle size index is examined below, further information about the source of the aerosols may be inferred. From Figure 2 it is seen that for a given radiance, when the particle size index decreases the phase function decreases. This leads to an increase in optical depth for most scattering angles. This is the case for the corrected optical depth in Figure 8. Here again a high optical depth is noted on the left periphery of the figure. It extends eastward into the upper and central areas of the figure. This may be due to dust intrusions from Asia. Another possibility for the increasing optical depth to the west is related to the retrieval process. This is the result of the satellite sensor's aperture moving to the left and to the right of the of the satellite's path to view side regions. The satellite is looking mainly at backscatter when it looks directly at the Earth. As the sensor looks to the side it is no longer viewing backscatter but smaller scattering angles. This results in a decrease in the phase function and a corresponding increase in the optical depth. This is an area that should be investigated further in future work.

Figure 9 shows Benedict's (1989) composite optical depth averaged geographically for all longitudes. There is a peak in the vicinity of 40°N indicating a potentially greater number of particles in the region. This could be a reflection of the advection of Asian particulates into the area. These could be natural dust or anthropogenic pollutants. There is another peak near 8°N. Since Figure 8 revealed little optical depth from the eruption of Kilauea, this peak is probably due to DMS production in the tropics.

The optical depths obtained from this study, shown together in Figure 10, reveal a profile with greater structure, especially in lower latitudes where there is a peak at 22°N not revealed by Benedict (1989). The peak at 6°N is also shifted north to near 10 °N. This shows possible error in the HG phase function parameterization. The increase in optical depth south of 20°S is subject to error as it is near the data set boundary. The values of optical depth are larger than those of Benedict due to the ozone correction. This correction increases channel one radiance resulting in a higher optical depth.

Figures 11 and 12 present the composite particle size index and particle size index corrected for water vapor for the entire experimental period. The uncorrected particle size index shows a plume in red extending westward from the Kilauea volcano. The higher particle size index indicates smaller particles. To the north in the midlatitudes is a darker area of blue indicating larger particles. This could be attributed to dust from the Asian continent being advected to the east. The large area of dark blue to the

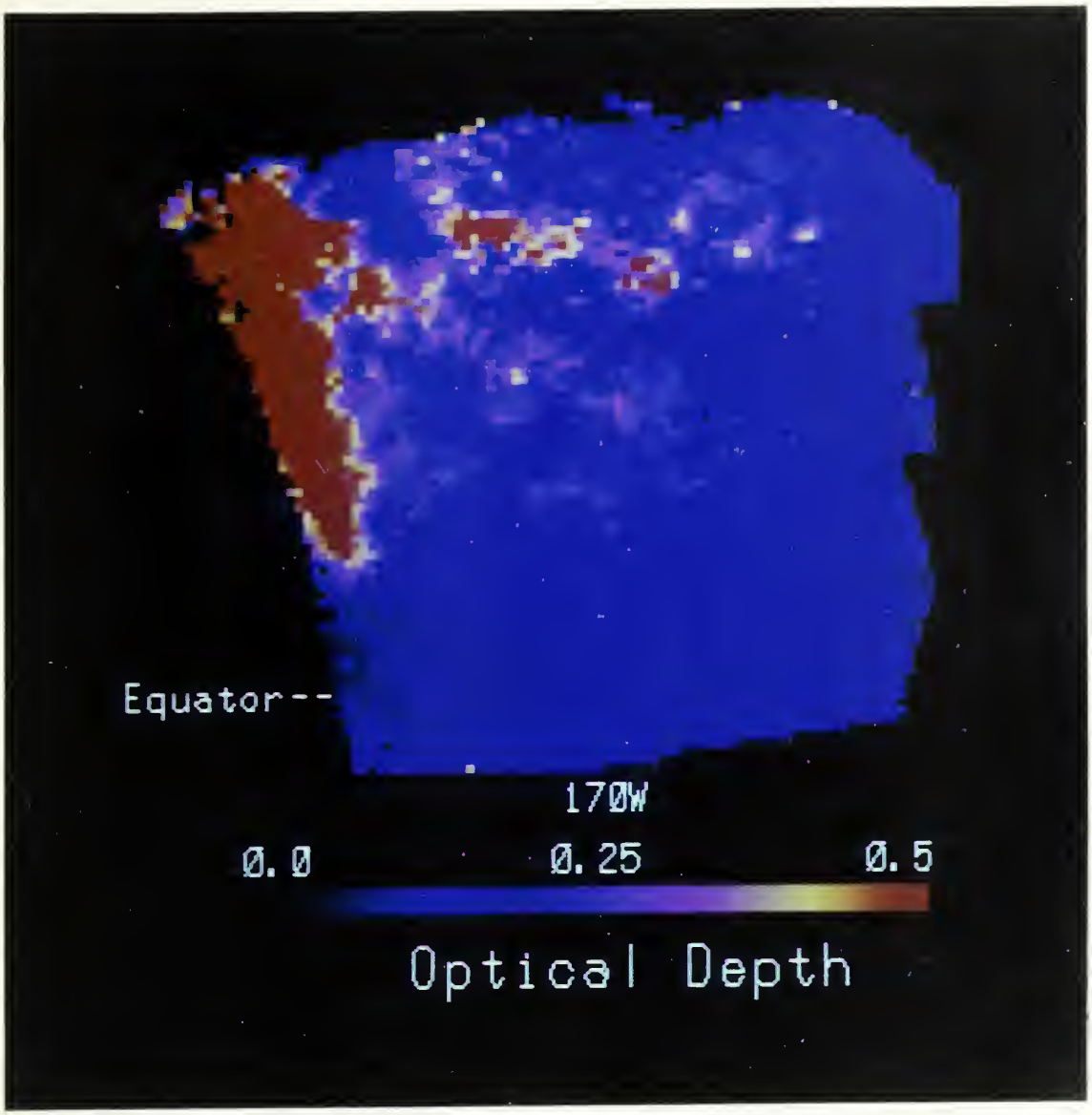

Figure 7. **Composite channel one optical depth:** the area extends from roughly 50 °N to 12°S and 162°E to 142°W.

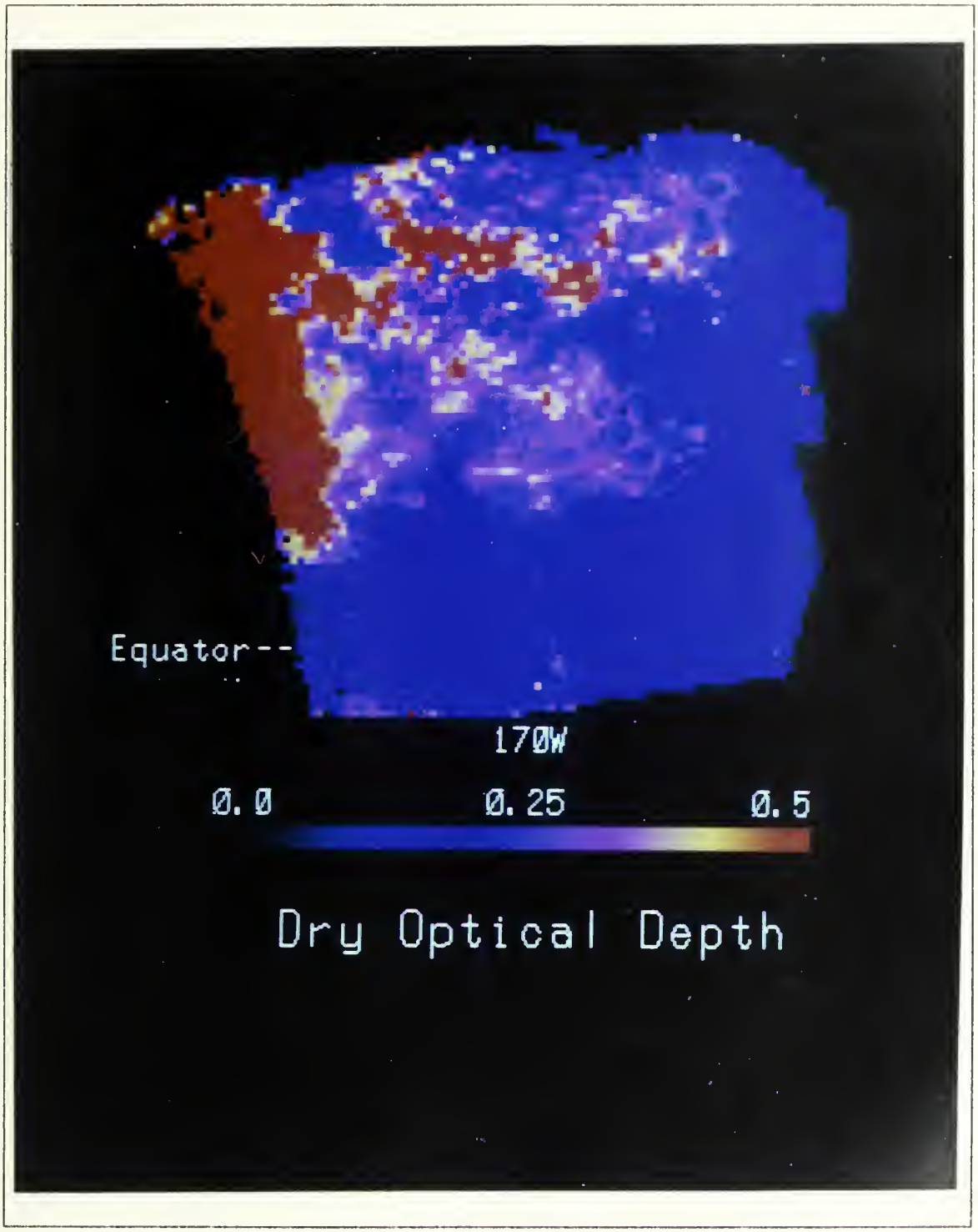

Figure 8. Dry composite channel one optical depth: the area extends from roughly 50°N to 12 ° S and 162°E to 142°W.

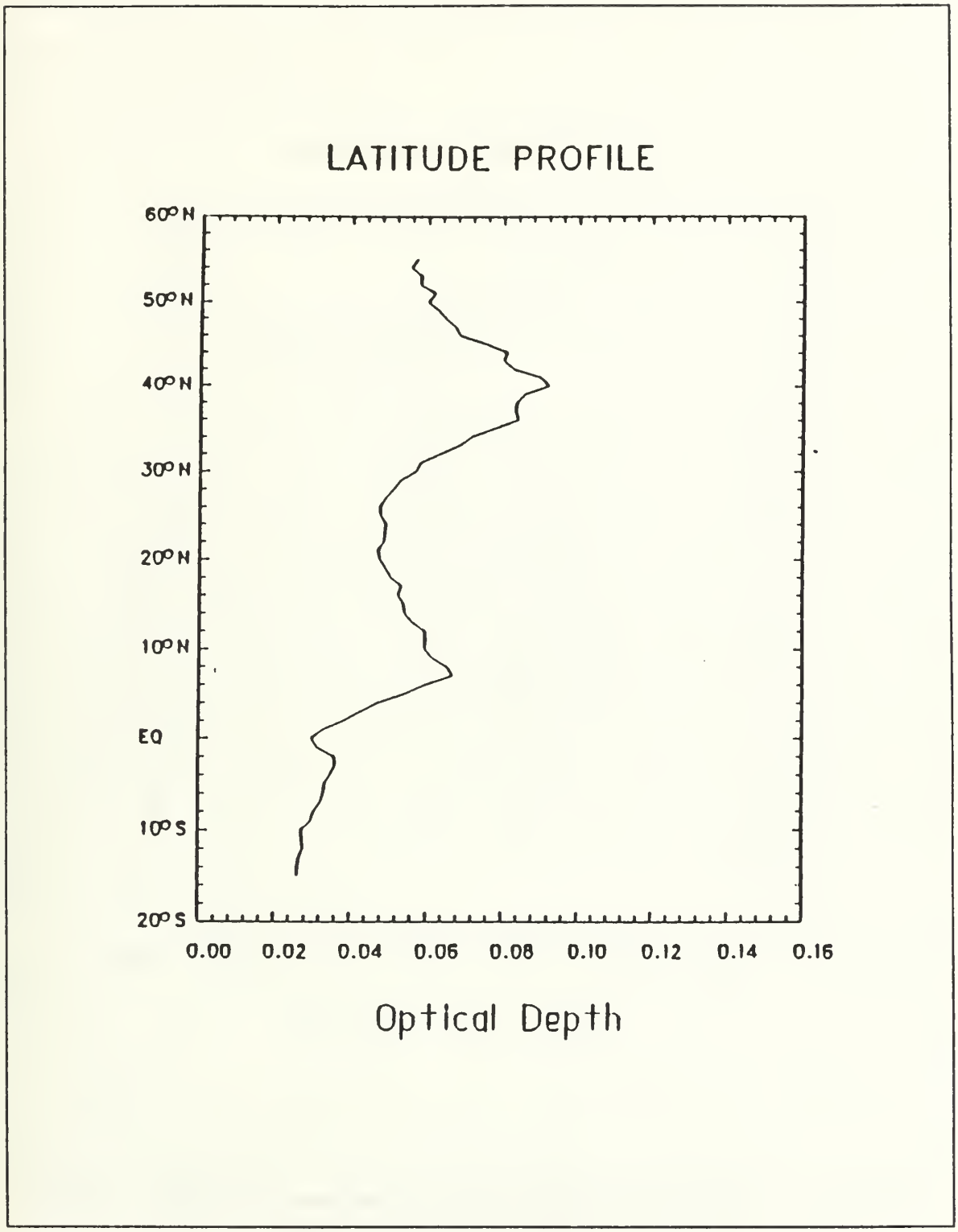

Figure 9. Composite channel one optical depth (Benedict 1989)

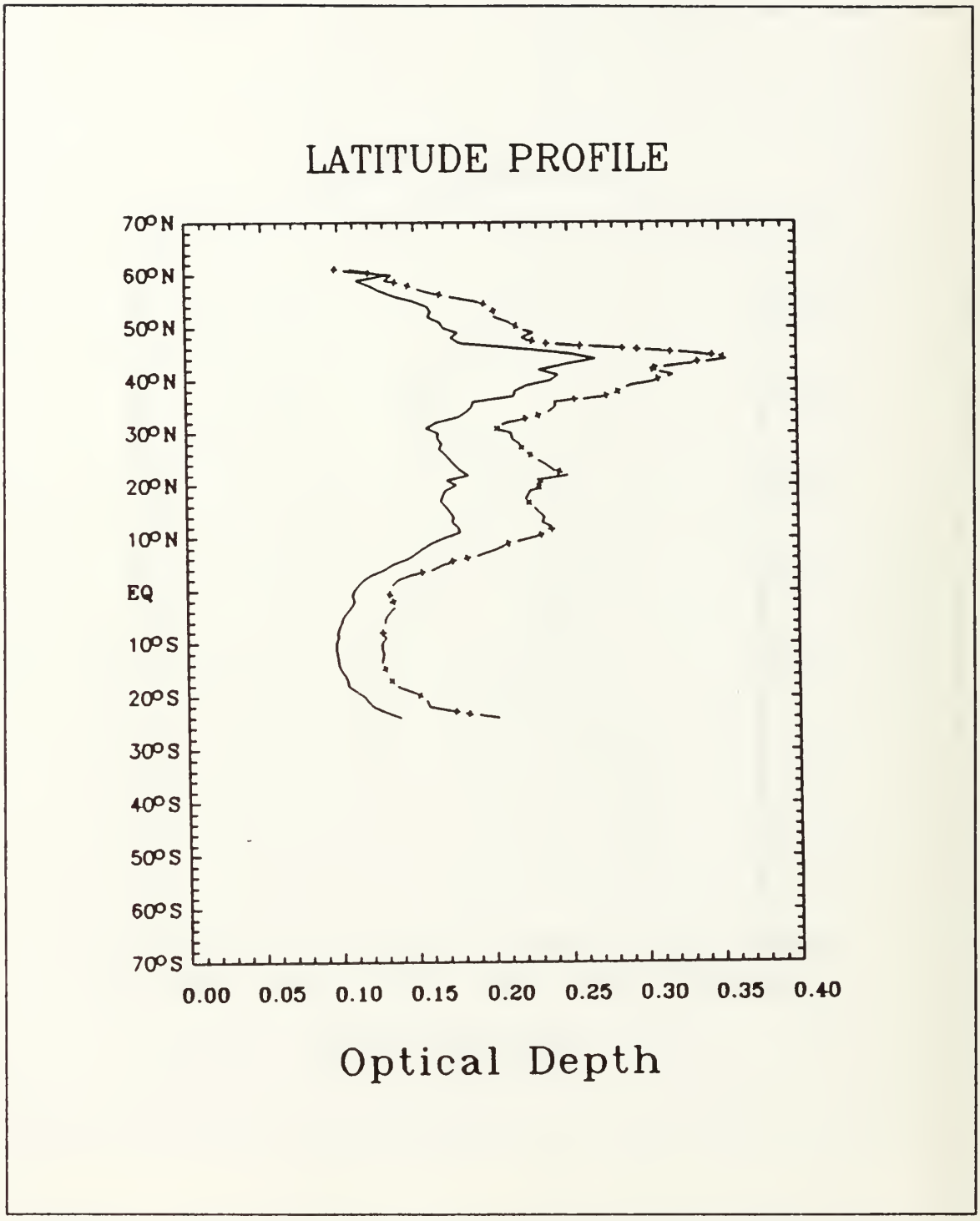

Figure 10. Composite uncorrected and dry channel one optical depth: the uncorrected values are smaller than the dry values.

western side of the image is unidentified although it could represent more dust. The somewhat lower particle size index on the left side of the figure might also be related to the retrieval process discussed above.

The particle size index corrected for water vapor, Figure 12, shows lower values. Since water vapor causes an overestimation of S_{12}, this was expected. Now the plume from Kilauea is less evident but the dust influence to the north is more significant.

Figure 13 shows the composite particle size index obtained by Benedict (1989). The results are averaged geographically for all longitudes. A peak in the neighborhood of 30-40°N is evident indicating possible influence by smaller particles being advected from the west. Another peak is noticed at about 6°N indicating smaller particles, possibly a result of DMS production in the tropics.

The plots of composite particle size index and dry particle size index for this study are both shown in Figure 14 for comparison. They show more structure and definition than the plot of Benedict (1989). The values are higher than those of Benedict (1989) due to the modifications in the algorithm. In Benedict's (1989) study ozone was over corrected for leading to a proportionately higher radiance in channel two and thus lower particle size indices. The uncorrected index is higher than the corrected index as before. Both curves show the midlatitude peak of Benedict (1989) but also show more of a peak in the tropical regions. The Benedict (1989) plot decreases toward the equator while the plots of this study increase. This supports the changes to the algorithm since the particle size index is expected to increase in the tropics because of higher DMS production. In addition, the dry index has a larger correction for the tropical regions due to the greater effect of water vapor there. The increase in S_{12} near 60°N may be due to a reduction of valid data near the edge of the area.

The next data sets are in an area of plus or minus five degrees of longitude from the ship's track and within plus or minus three days of the ship's position which limits the data used in the north-south direction. This is to get a better comparison with the in-situ measurements.

Optical depth near the ship's track from Benedict (1989) is shown in Figure 15. A large double peak at about 40°N is evident with a smaller peak at about 33°N. In Figure 16 this study shows the same peaks at midlatitudes but also a large peak at 22°N. This is most likely due to volcanic particles which may have been averaged out in the previous composite (Figure 10) which included the entire data set. The corrected optical depths on the same plot are even larger. Higher optical depths were expected due to both the water vapor correction to the particle size index and the ozone correction. The optical

Figure 11. Composite particle size index: the area extends from roughly 50°N to 12°S and 162°E to 142°W.

Figure 12. Dry composite particle size index: the area extends from roughly 50°N to 12°S. and 162°E to 142°W.

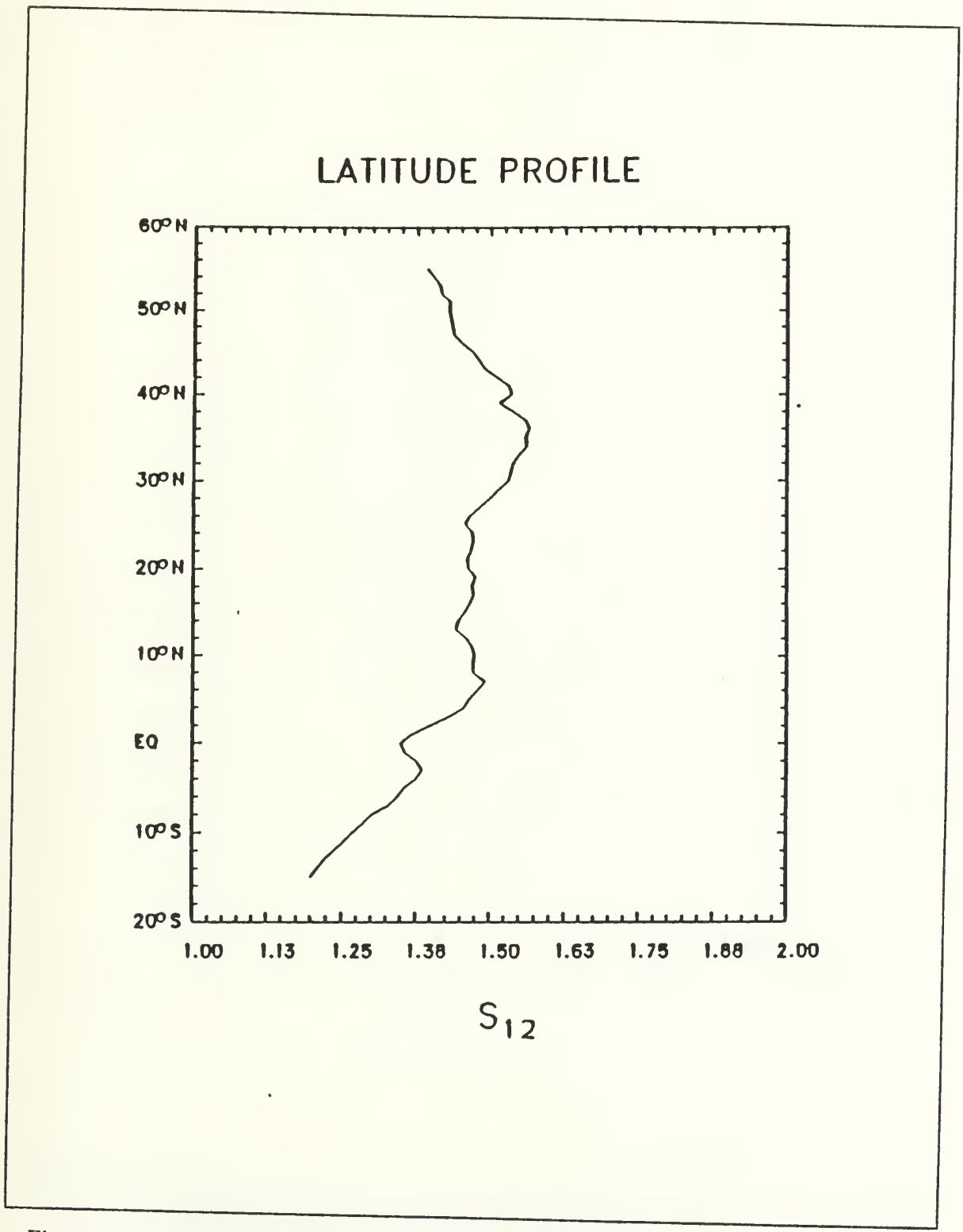

Figure 13. Composite particle size index (Benedict 1989)

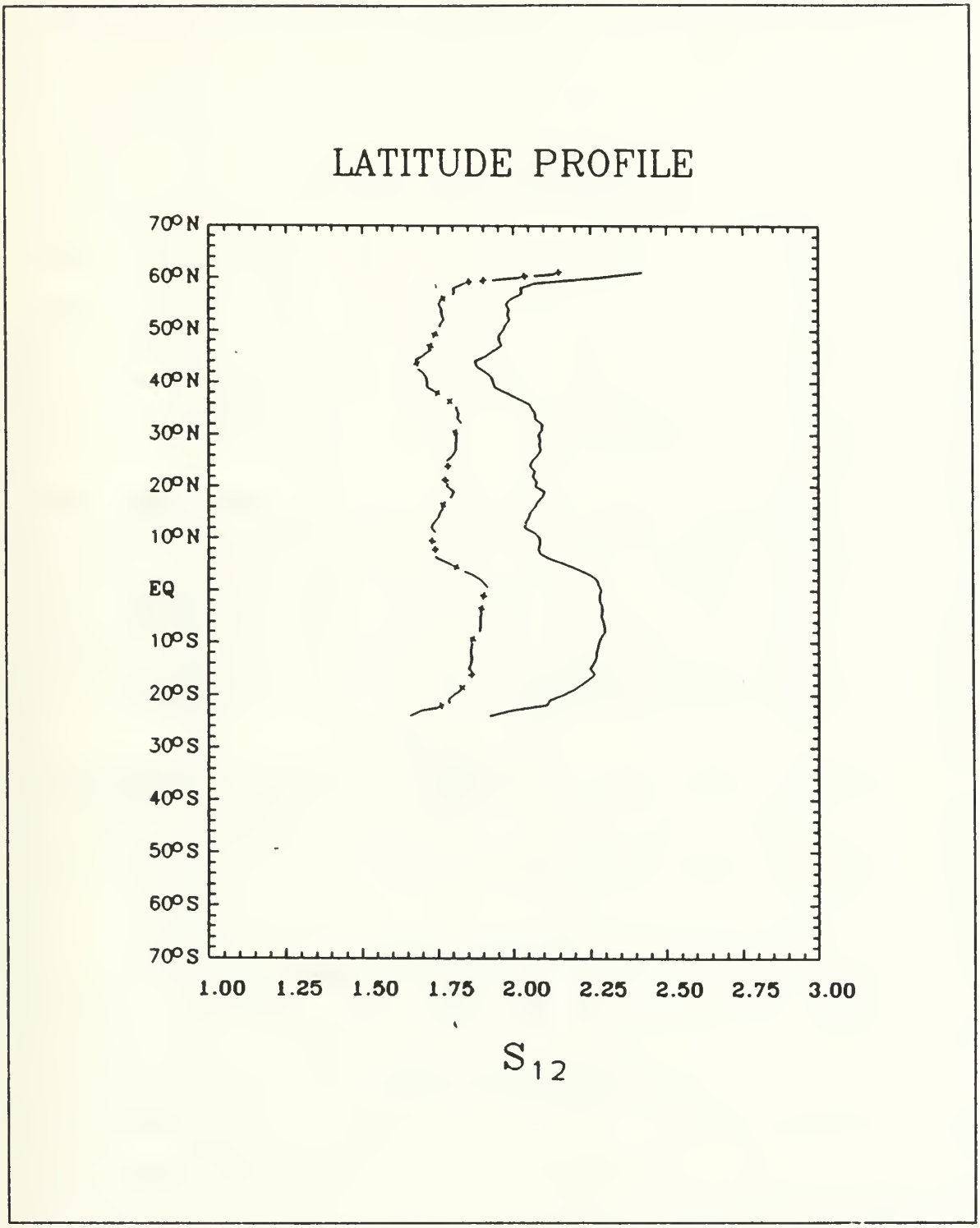

Figure 14. Composite uncorrected and dry particle size index: The uncorrected values are larger than the corrected values.

depth measured by a hand-held sun photometer on the ship is also plotted on Figures 15 and 16. Note that optical depth is scaled differently in the two figures. The magnitude of the optical depths obtained in this study appear to be supported by the photometer measurements. This indicates support for the corrections made to the algorithm. There appears to be a northward shift of about 5-7° in the satellite estimated optical depth compared to the ship measurements. This could be caused in part by the way the data is averaged by three days around the ship's track. It is possible that satellite data within one day of the ship's track would produce better results. The reason this wasn't done was to ensure enough data were available to fill in times when cloudy pixels were thrown out. A second reason for the shift may be due to inaccuracies in the positioning of either the ship or satellite data and a third alternative is that the parameterization of the HG phase function is incorrect. Changes to improve the phase function are discussed below.

In-situ measurements of condensation nuclei are shown in Figure 17 although they too are shifted several degrees south of the satellite data. The condensation nuclei are not the same as CCN, CCN are a subset of the condensation nuclei, being the condensation nuclei capable of nucleating with water vapor to form cloud droplets. However, for the purpose of optical depth measurement they can be treated similarly. Another peak not resolved by Benedict's (1989) or this data set is evident at 6 and 12°S.

Figure 18 from Benedict (1989) shows the particle size index in the neighborhood of the ship's position. It is a little more definitive than the previous composite and reveals a midlatitude peak around 30-40°N, another at about 20°N, and another near 10°N. A distinction can be made between an influence from Kilauea volcano at 20°N and DMS production leading to non-sea-salt sulfate aerosols near the equator.

Figure 19 shows the combined uncorrected and dry particle size index near the research vessel's track for this study. The peaks are more pronounced than Benedict (1989) and there is a minimum at 22°N. where Benedict (1989) shows a peak. The values of S_{12} are higher overall and the difference between uncorrected and dry particle size index is larger near the equator. There is also an increase in the results moving south of the equator as well as a peak not seen in the Benedict (1989) results, possibly due to DMS production.

Next, the non-sea-salt sulfate data obtained from the *R/V Oceanographer* are plotted in Figure 20. Here there is a peak clearly evident centered at about 20°N. This is strong indication of smaller particles, most likely from the volcanic fallout. These results point

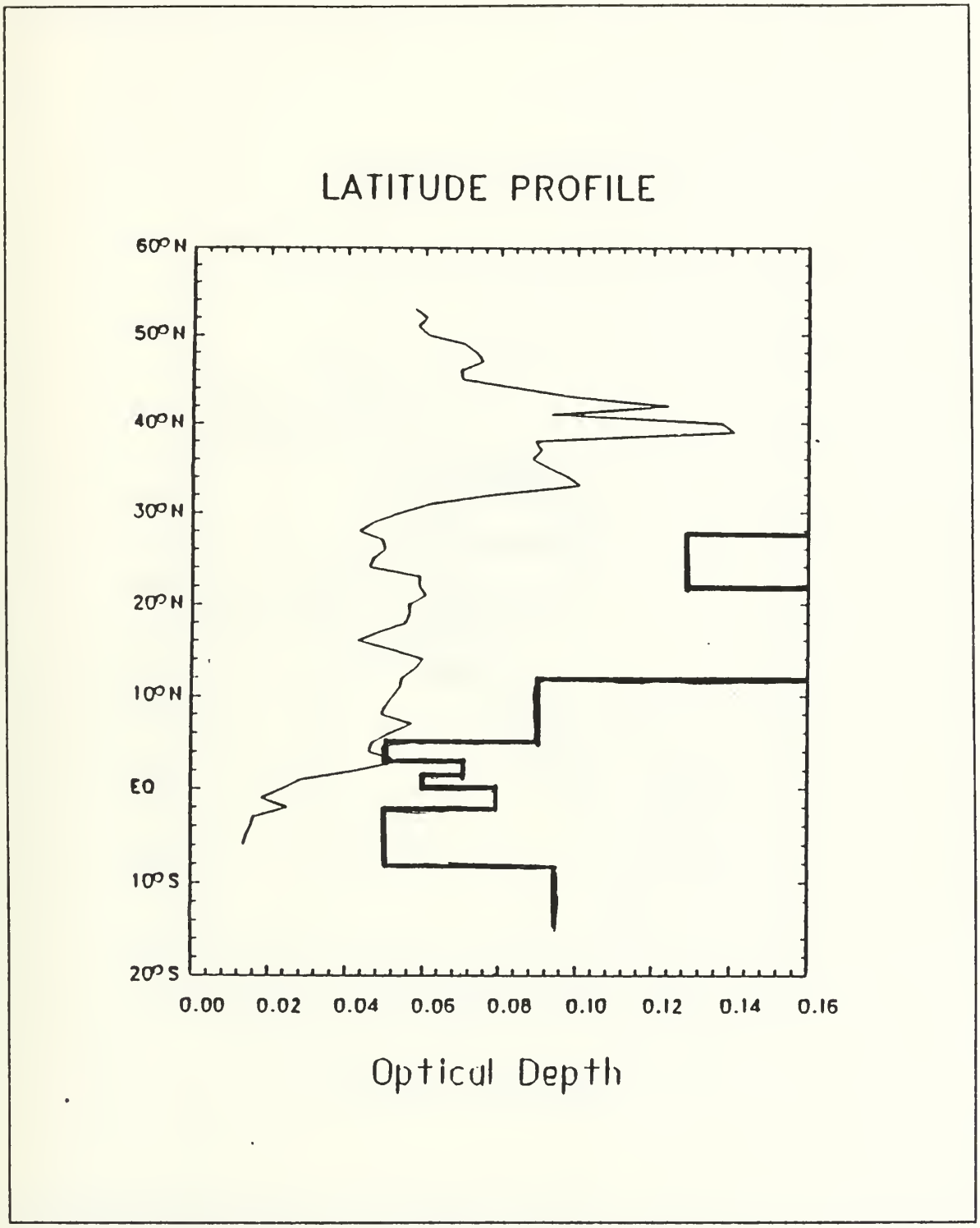

Figure 15. Channel one optical depth along ship's track (Benedict 1989): photometer measurements superimposed.

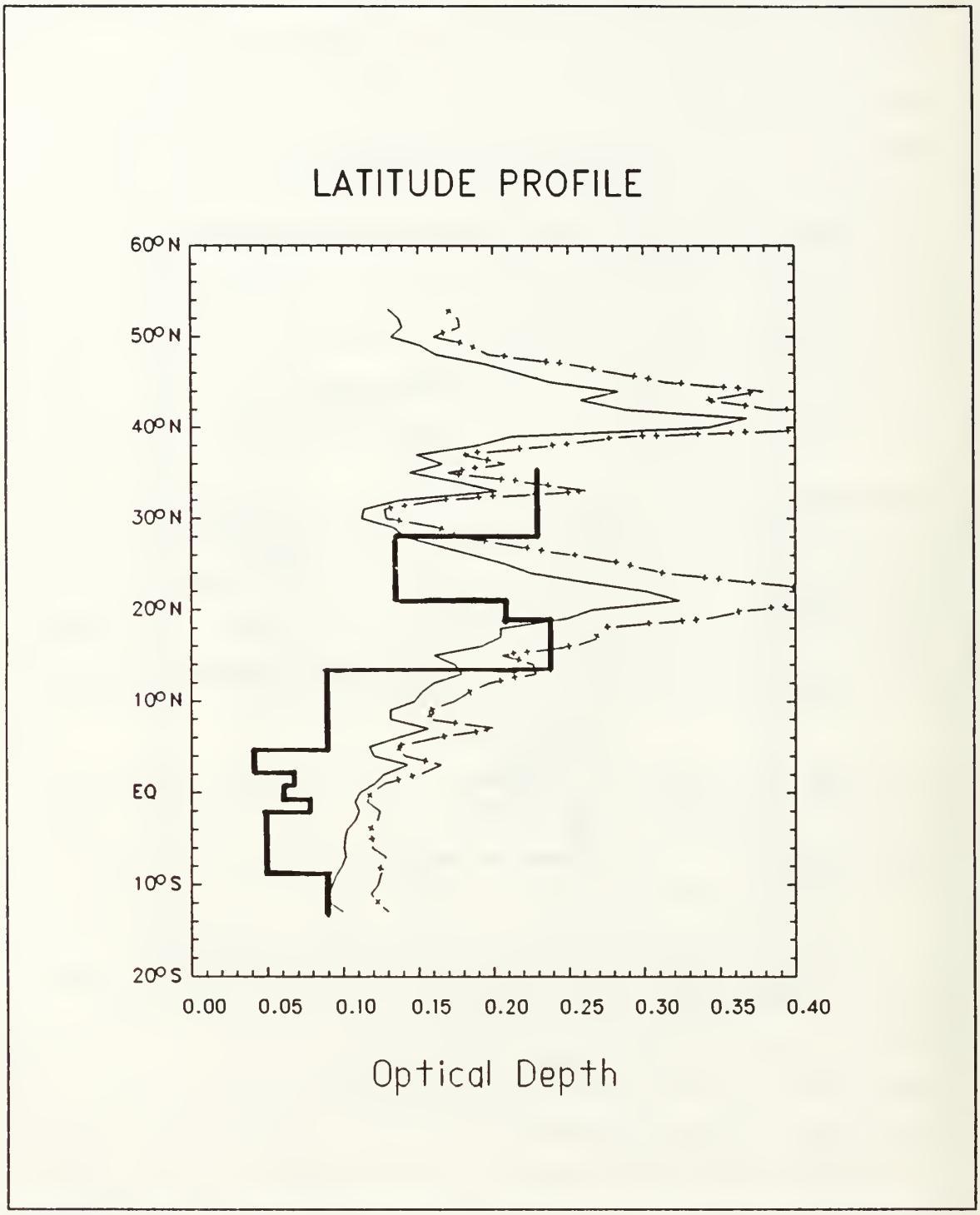

Figure 16. Uncorrected and dry channel one optical depth along ship's track: photometer measurements superimposed

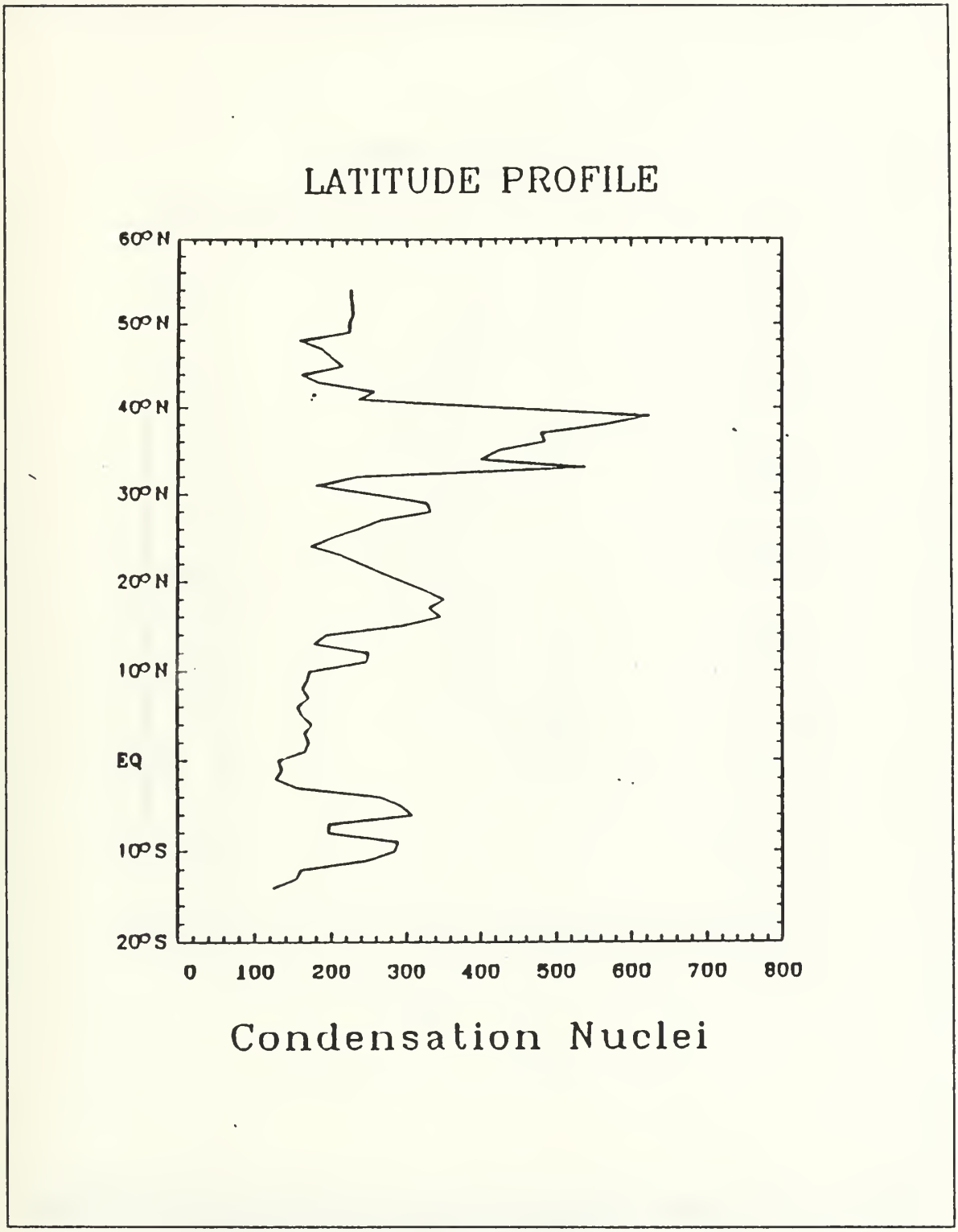

Figure 17. Condensation nuclei along ship's track (Benedict 1989)

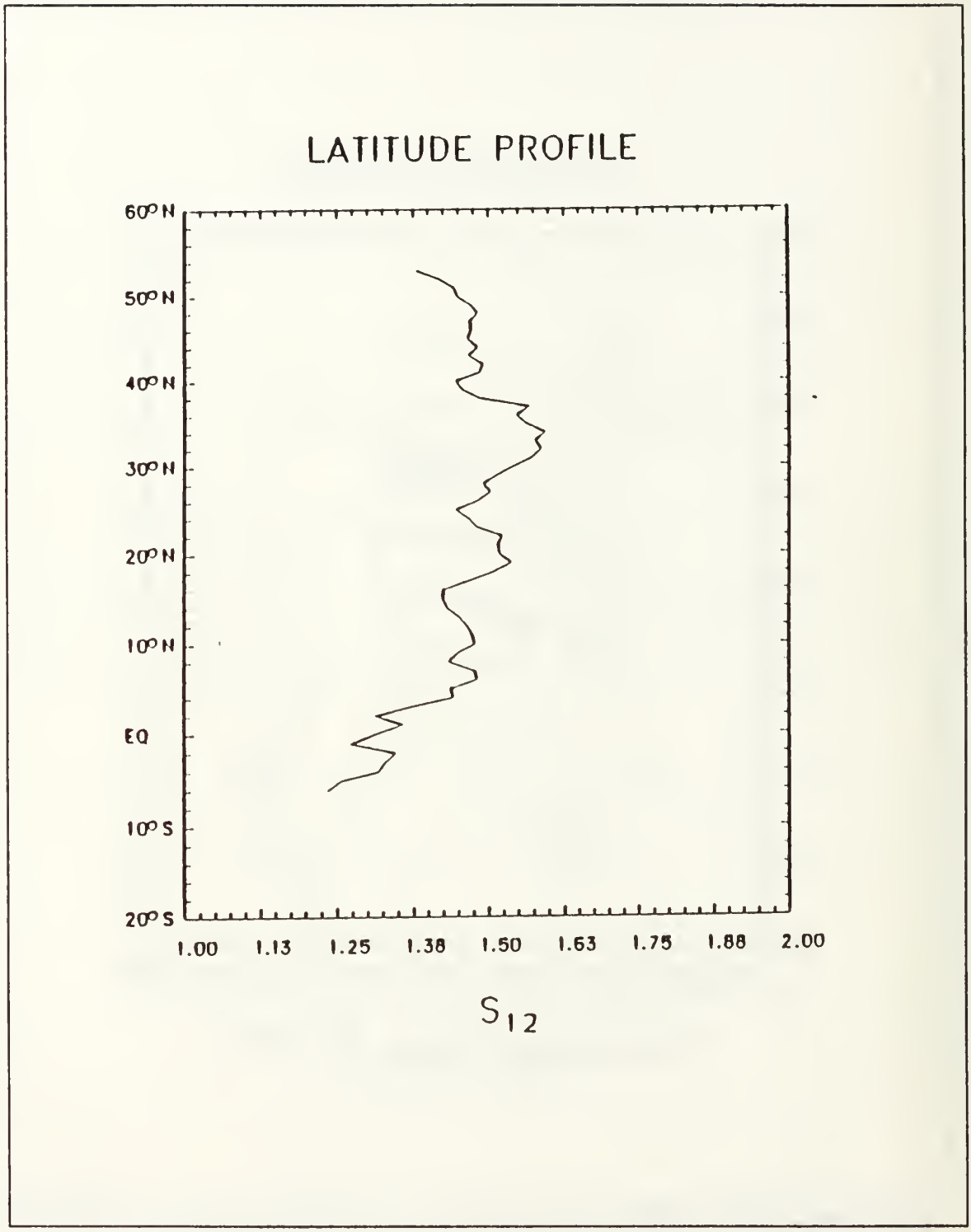

Figure 18. Particle size index along ship's track (Benedict 1989)

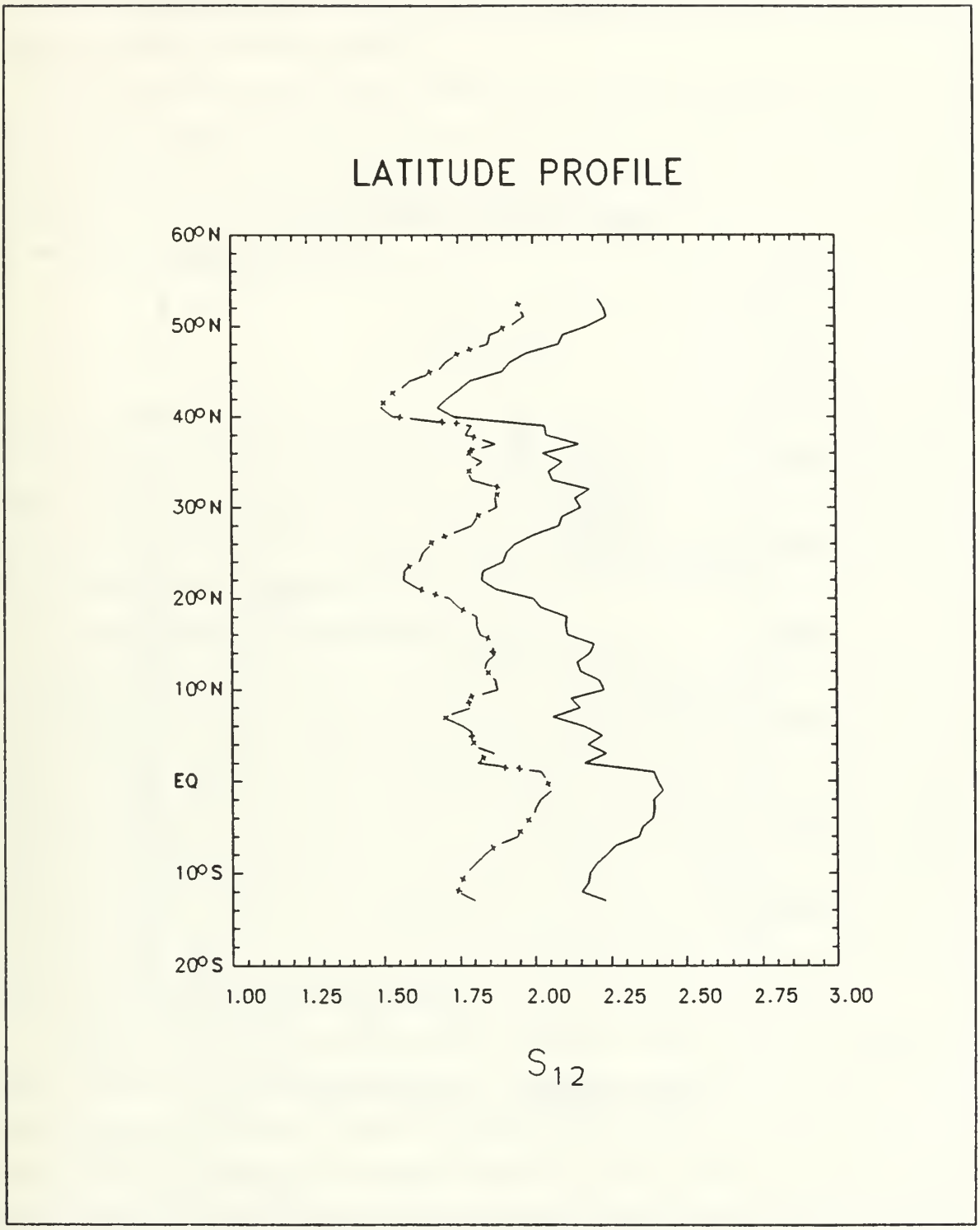

Figure 19. Uncorrected and dry particle size index along ship's track: the uncorrected values are larger than the dry values.

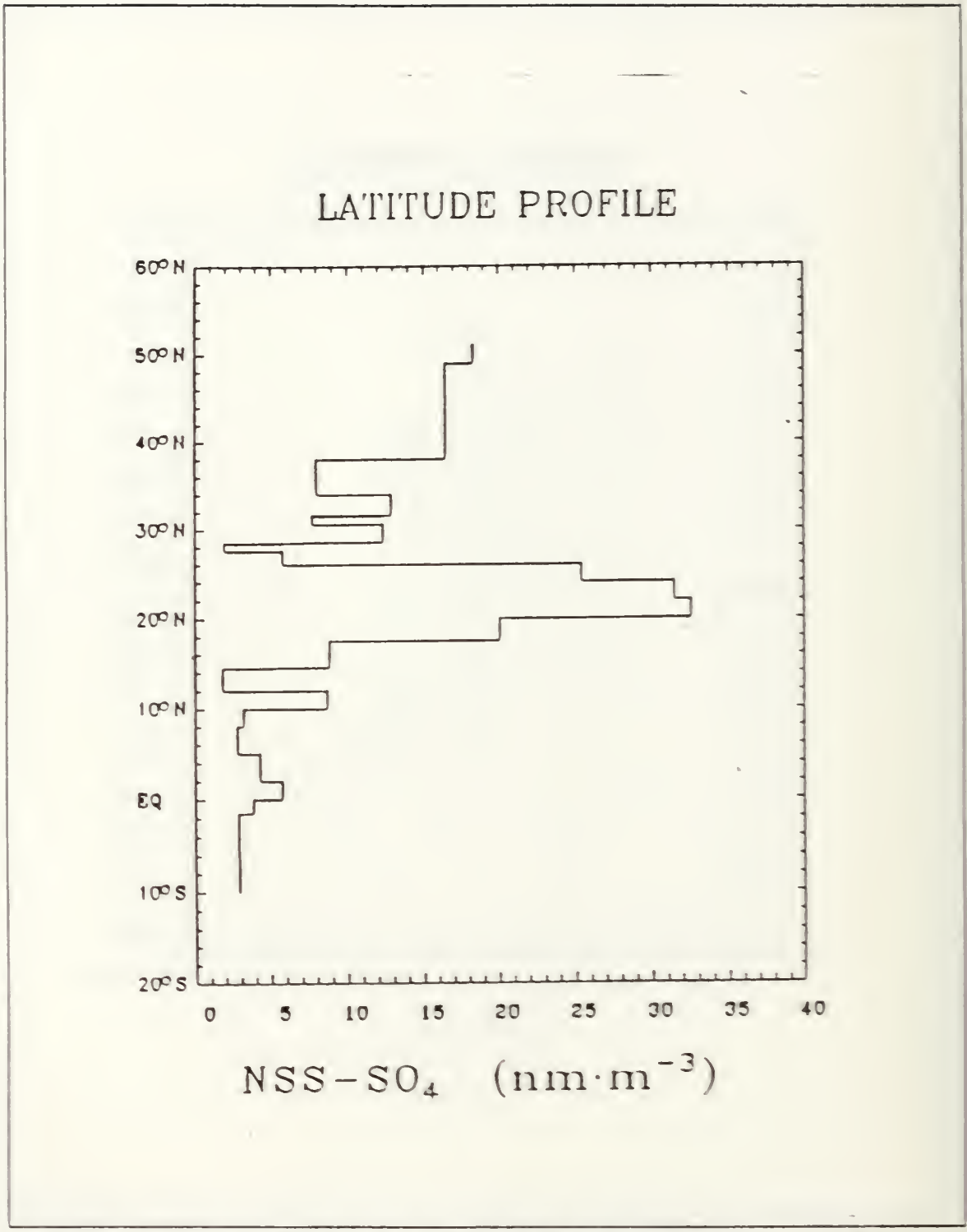

Figure 20. Non-sea-salt sulfate along ship's track (Benedict 1989)

to errors in the phase function parameterization since there is no corresponding peak in particle size index as would be expected.

The next plot to be studied is the geometry variable used to examine the correlation between optical depth and phase function. By plotting the normalized measured radiance as a function of scattering angle for various particle size indices, any correlation between the phase function and particle size index is separated out. This can be seen by rearranging equation 2.4 to give

$$P = \frac{L4\mu}{\omega_o F_o} = p(\Theta)\delta.$$

The left hand side represents values that are all measured or known while the two terms on the right must be parameterized (the phase function) or calculated (the optical depth). By using the optical depth that best fits the data for a given measured particle size index, the phase function can be adjusted and improved. The phase function used by Frost (1988) and Benedict (1989) was simply one way, not necessarily the best way for this data, of parameterizing the phase function.

The results of P versus Θ are shown in Figure 21 and can be compared to Figure 2, the HG phase function. To make an accurate comparison, the HG phase function used by Frost (1988) should be multiplied by a mean optical depth. This is done for two values of the particle size index in Figure 22 and allows for a direct comparison between the HG phase function and study results. For a particle size index of 1.7, the HG phase function was multiplied by a mean optical depth of 0.2 and for a particle size index of 2.1, the HG phase function was multiplied by a mean optical depth of 0.1. These values of mean optical depth are only approximate. Further evaluation of the study results would be required for more accurate values.

The shapes of both curves are similar but in the area of 0-20° scattering angle the results of this study are up to three orders of magnitude lower. This is due partly to the observations in the 0-60° bin. Most of the pixels in this bin have a scattering angle between 50 and 60° resulting in a P weighted toward the lower values of the higher scattering angles. The total number of pixels evaluated for this bin was also less than the other bins potentially contributing to an unrepresentative P in this area. For the particle size of 1.7 in this study, there also appears to be a shift in minimum P values toward higher scattering angles than for the HG phase function.

By adjusting phase function parameters a better fit can be obtained. In Figure 23, after multiplying the HG phase function by a mean optical depth of 0.15 and using the $S_{12} = 1.7$ data curve, the following values from equation 2.8 were obtained: α was set to 0.95, g_1 and g_2 were set to 0.5. In this way the form of α, g_1, and g_2 can be determined.

Another aspect of the problem is that the results were always obtained using the HG phase function parameterization for channel one. Channel two results are also available but they are computed using the phase function for channel one. The phase function is wavelength dependent and could result in some error for channel two calculations. Using the same procedure as above but for channel two, it should be possible to derive a channel two correction to the Henyey-Greenstein phase function. This would result in knowing all parameters in the simplified RTE except optical depth, which could then be calculated directly for either channel. A new particle size ratio of optical depths from channels one and two would then more directly measure particle size information.

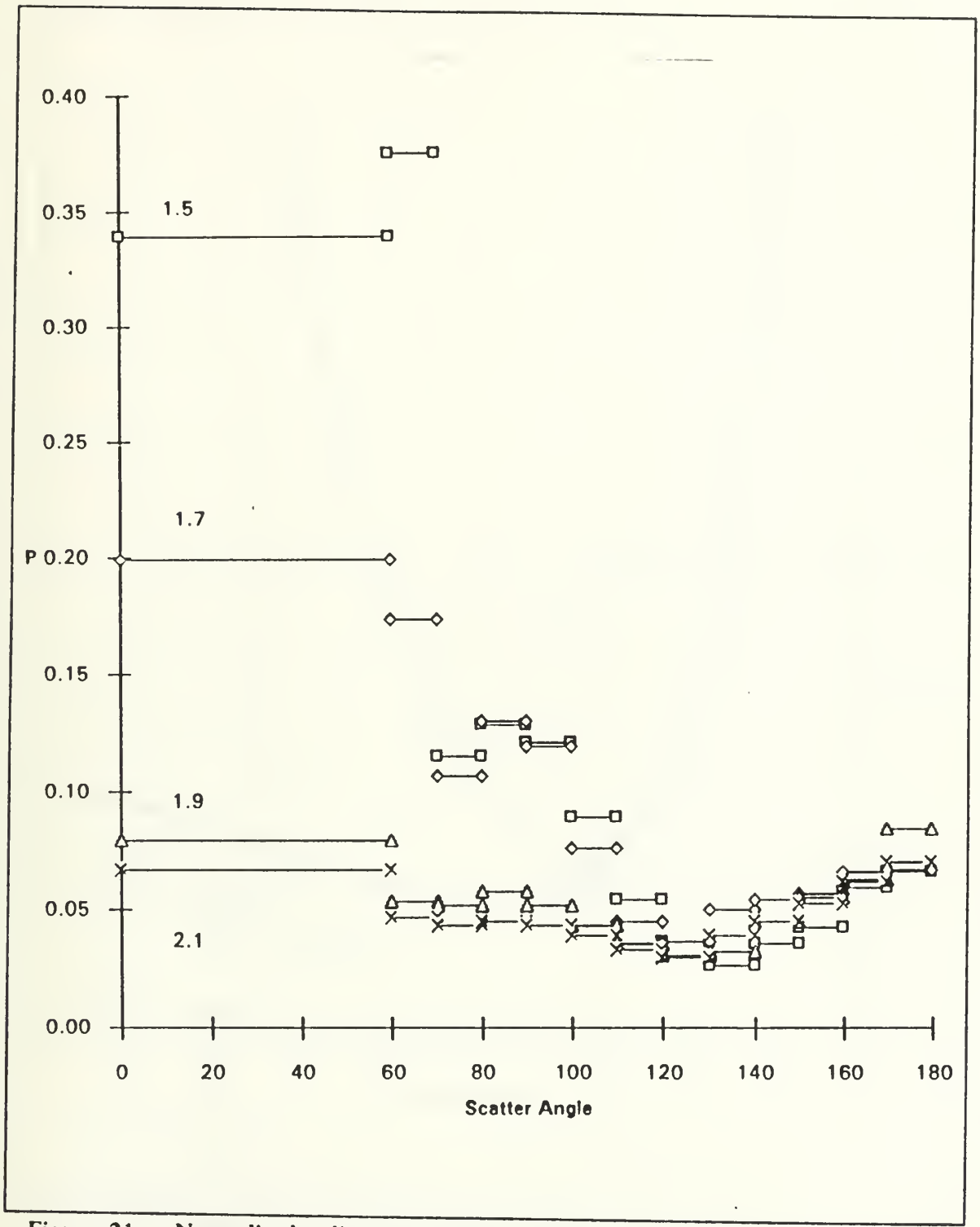

Figure 21. Normalized radiance (P) versus scattering angle (Θ): for various S_{12}.

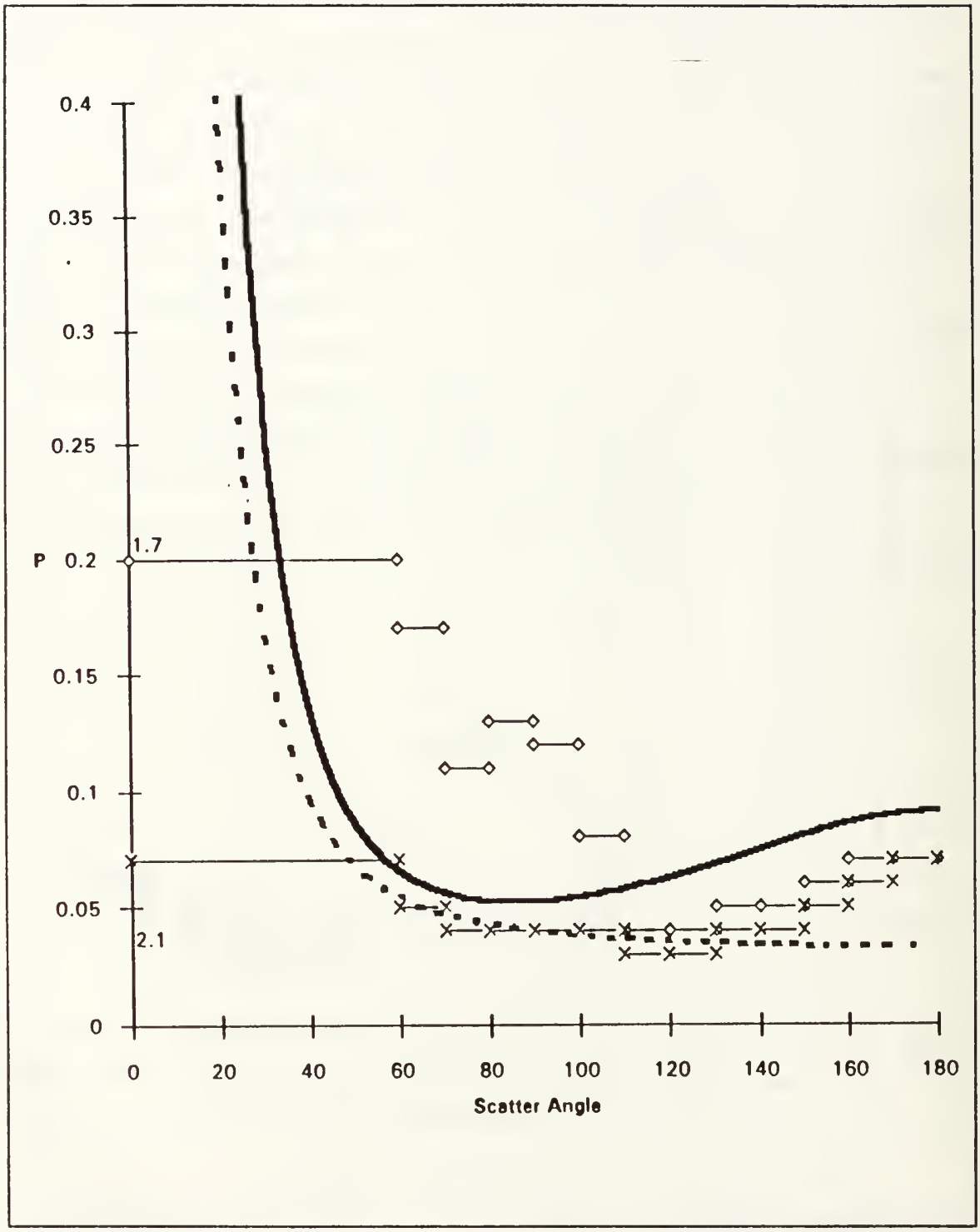

Figure 22. Scaled HG phase function and P versus Θ: for particle size index of 1.7 (solid line) and 2.1.

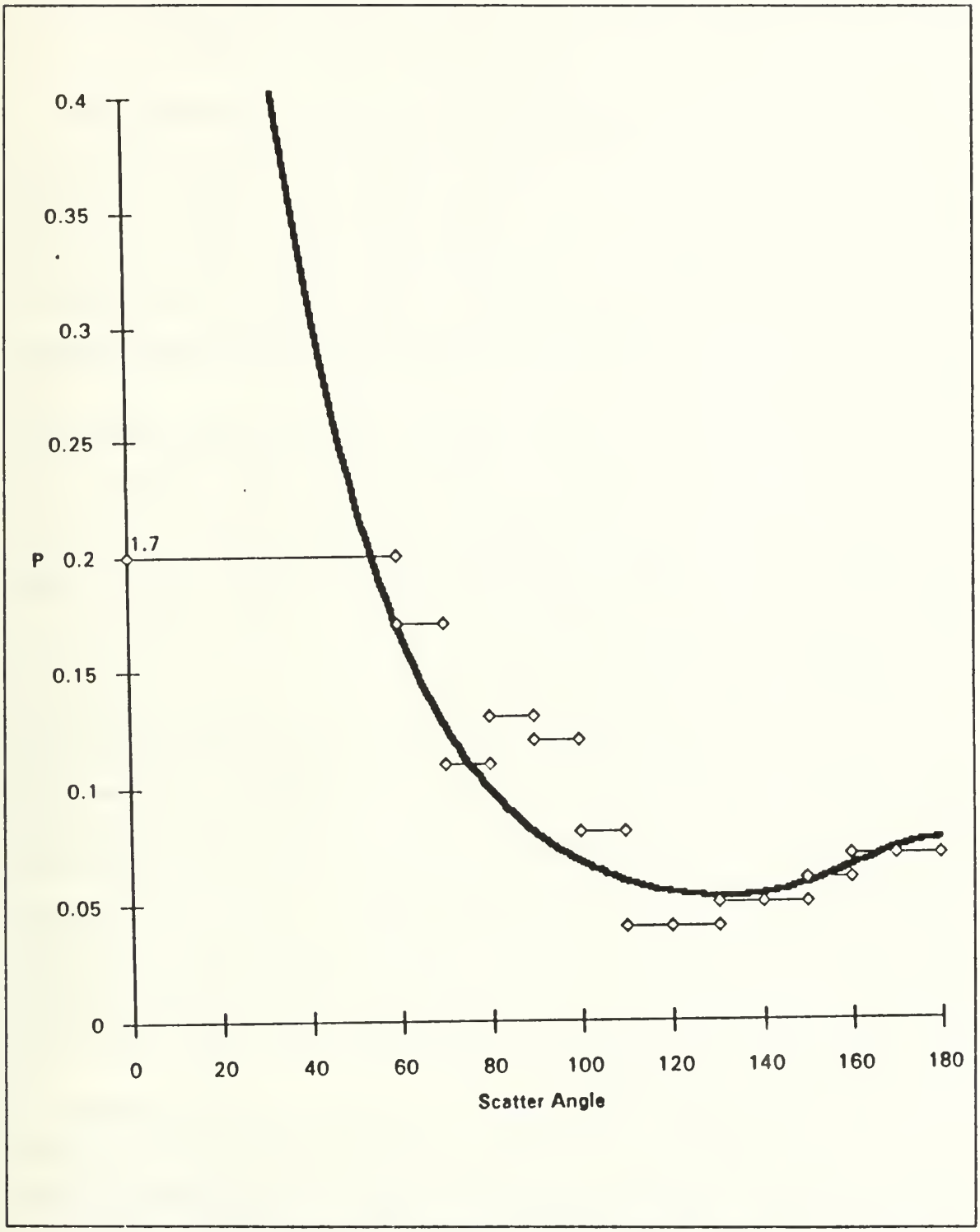

Figure 23. **Scaled and adjusted HG phase function and P versus Θ:** for a particle size index of 1.7.

V. CONCLUSIONS AND RECOMMENDATIONS

This study examined an algorithm that extracts aerosol particle size index and optical depth from satellite observations of upwelling radiance over clear ocean areas. By utilizing the difference in sensitivity between channels, particle size information is measured and optical depth can then be calculated. Data retrieved from the NOAA-9 AVHRR sensor was reanalyzed and compared to shipboard measurements made by the *R/V Oceanographer* during the RITS-88 cruise. In this fashion the satellite retrieval technique is verified and our understanding of marine aerosols on a regional scale is increased.

This study improved upon the results of Benedict (1989) after making corrections to account for variable earth-sun distance on solar irradiance, making an adjustment for a previous over correction to ozone absorption and correcting the computer code for a mathematical error. These combined corrections had a greater effect on the results than anticipated. The direction of the corrections was positive, however. An improvement to the algorithm, which takes into account the absorption of column water vapor, was examined and also found to improve the results.

Finally, the correlation between aerosol optical depth and the Henyey-Greenstein phase function was examined. It was concluded from the plots of P versus Θ for various particle size indices that some correlation did exist. An adjustment to one case of the HG phase function was made with excellent results. It is recommended to calculate a new set of phase functions that fit the experimental data. This would account for the correlation between optical depth and scattering angle thus making optical depth and phase function independent of one another. Then optical depth could easily be calculated and a ratio of optical depths would be a new, more accurate particle size index. This is because the slope of the particle size distribution, which is part of optical depth, would be more directly compared.

Another recommendation of this study is to separately calculate a correction to the HG phase function for channel two. Then the channel two phase function could be used in the calculations of channel two optical depth instead of the channel one phase function. It is also recommended that the simplified RTE be adjusted for multiple scatter. The single scattering approximation is good up to an optical depth of about 0.1. The results obtained show that the optical depths were higher than 0.1 leading to errors in

the results. Other regional studies should be undertaken to continue examining and improving the algorithm and its performance. Global scale studies are also useful but it is less likely that there will be in-situ data available for verification.

While this procedure appeared effective in revealing variations in aerosols in the region of interest for known sources, it appeared to have only moderate sensitivity to the NSS-SO_4^{2-}'s of interest. This makes studying DMS and its role in global climate regulation more difficult. It is therefore important that improvements to the algorithm continue to be made. As discussed by Benedict (1989), studying areas where there is less interference from natural or human-made sources is one possibility as is studying regions of higher phytoplankton activity, such as the tropics. Additional satellite-inferred aerosol studies are required to guide future algorithm improvements and to provide critically needed measurements of global aerosol behavior.

LIST OF REFERENCES

Benedict, T.D., 1989: Satellite observations of aerosol variations in the central North Pacific Ocean. M.S. Thesis, Naval Postgraduate School, Monterey, CA., 53pp.

Charlson, R.J., and M.J. Pilat, 1969: Climate: the influence of aerosols. *J. Appl. Meteor.*, **8**, 1001-1002.

Charlson, R.J., J.E. Lovelock, M.O. Andreae, and S.G. Warren, 1987: Oceanic phytoplankton, atmospheric sulphur, cloud albedo and climate. *Nature*, **326**, 655-661.

Charlson, R.J., and T.S. Bates, 1989: The role of the sulfur cycle in cloud microphysics, cloud albedo, and climate. *Symposium on the Role of Clouds in Atmospheric Chemistry and Global Climate*, Preprints, 1-3.

Coakley, J.A., R.D. Cess, and F.B. Yurevich, 1983: The effect of tropospheric aerosols on the Earth's radiation budget: a parameterization for climate models. *J. Atmos. Sci.*, **40**, 116-138.

Cox, C.C., and W. Munk, 1954: Measurement of the roughness of the sea surface from the photographs of the Sun's glitter. *Journal of the Optical Society of America*, **44**, 838-850.

Dalu, G., 1986: Satellite remote sensing of atmospheric water vapor. *Intl. J. Remote Sensing*, **7**, 1089-1097.

Durkee, P.A., 1984: The relationship between marine aerosol particles and satellite detected radiance. Ph.D. Dissertation, Colorado State University, Fort Collins, CO., US ISSN 0067-0340, 124pp.

Durkee, P.A., D.R. Jensen, E.E. Hindman, and T.H. Vonder Haar, 1986: The relationship between marine aerosol particles and satellite detected radiance. *J. Geophys. Res.*, **91 D-3**, 4063-4072.

Durkee, P.A., F. Pfeil, E. Frost, and R. Shema, 1991: Global analysis of aerosol particle characteristics. *Atmospheric Environment*, **25 A**, 2547-2471.

Frost, E.M., 1988: Global scale estimates of aerosol particle characteristics. M.S. Thesis, Naval Postgraduate School, Monterey, CA., 54pp.

Griggs, M., 1975: Measurements of atmospheric optical thickness over water using ERTS-1 data. *Journal of Atmospheric Pollution Control Association*, **25**, 622-626.

Hindman, E.E., P.A. Durkee, P.C. Sinclair, and T.H. Vonder Haar, 1984: Detection of marine aerosol particles in coastal zones using satellite imagery. *Intl. J. Remote Sensing*, **5**, 577-586.

Kidwell, K.B., 1986: *NOAA Polar Orbiter Data Users Guide*. NOAA NESDIS National Climatic Data Center, Satellite Data Service Division, 145pp.

Lenoble, J., 1985: *Radiative Transfer in Scattering and Absorbing Atmosphere: Standard Computational Procedures.* A. Deepak Pub., 300pp.

Liou, K.N., 1980: *An Introduction to Atmospheric Radiation.* Academic Press, 392pp.

Lovelock, J.E., 1986: Geophysiology: a new look at Earth Science. *Bull. Am. Met. Soc.*, **67**, 392-397.

Mahony, T.P., 1991: Water vapor influence on satellite-measured aerosol characteristics. M.S. Thesis, Naval Postgraduate School, Monterey, CA., 43pp.

McCormick, R.A., and J.H. Ludwig, 1967: Climate modification by atmospheric aerosols. *Science*, **156**, 1358-1359.

Mooradian, G.C., 1981: Surface and subsurface optical communications in the marine environment. *Optical Engineering*, **20** , 71-75.

Painter, F.C., 1989: Submarine laser communications. *Defense Electronics*, **:21**(6), 82-94.

Pfeil, F.R., 1986: Developing a physical basis for an aerosol climatology of the Pacific Ocean. M.S. Thesis, Naval Postgraduate School, Monterey, CA., 75pp.

Ramsey, R.C., 1968: Study of the remote measurement of ocean color. Final Report, TRW, NASW-1658.

Rao, P.K., S.J. Holmes, R.K. Anderson, J.S. Winston and P.E. Lehr, Eds., 1990: *Weather Satellites: Systems, Data, and Environmental Applications.* American Meteorological Society, 503pp.

Shaw, G.E., 1980: Transport of Asian desert aerosol to the Hawaiian Islands. *J. Appl. Meteor.*, **20**, 1254-1259.

Shaw, G.E., 1983: Bio-controlled thermostasis involving the sulfur cycle. *Climatic Change*, **5**, 297-303.

Shettle, E.P., and R.W. Fenn, 1979: *Models for the Aerosols of the Lower Atmosphere and the Effects of Humidity Variations on their Physical Properties.* AFGL-TR-79-0214 Air Force Geophysics Laboritories, Hanscom AFB, MA.

Turner, R., 1973: Atmospheric effects in remote sensing, *Remote Sensing of Earth Resources, II* (F. Shahrockhi, Ed.). University of Tennessee, 549-583.

Twomey, S.A., 1977: The influence of pollution on the shortwave albedo of clouds. *J. Atmos. Sci.*, **34**, 1149-1152.

Twomey, S.A., M. Piepgrass, and T.L. Wolfe, 1984: An assessment of the impact of pollution on global cloud albedo. *Tellus*, **36 B**, 356-366.

INITIAL DISTRIBUTION LIST

		No. Copies
1.	Defense Technical Information Center Cameron Station Alexandria, VA 22304-6145	2
2.	Library, Code 52 Naval Postgraduate School Monterey, CA 93943-5002	2
3.	Chairman (Code OC/Co) Department of Oceanography Naval Postgraduate School Monterey, CA 93943-5000	1
4.	Chairman (Code MR/Hy) Department of Meteorology Naval Postgraduate School Monterey, CA 93943-5000	1
5.	Professor P.A. Durkee (Code MR/De) Department of Meteorology Naval Postgraduate School Monterey, CA 93943-5000	1
6.	Professor C.H. Wash (Code MR/Wx) Department of Meteorology Naval Postgraduate School Monterey, CA 93943-5000	1
7.	Mr. Craig E. Motell Department of Meteorology Naval Postgraduate School Monterey, CA 93943-5000	1
8.	Mr. Brian H. Miller 1290 Seventh Street, Apartment 2 Monterey, CA 93943-3655	1
9.	Director Naval Oceanography Division Naval Observatory 34th and Massachusetts Avenue NW Washington, DC 20390	1
10.	Commander Naval Oceanography Command Stennis Space Center MS 39529-5000	1

11. Commanding Officer 1
Naval Oceanographic Office
Stennis Space Center
MS 39529-5000

12. Commanding Officer 1
Fleet Numerical Oceanography Center
Monterey, CA 93943-5005

13. Commanding Officer 1
Naval Oceanographic and Atmospheric Research Laboratory
Stennis Space Center
MS 39529-5004

Thesis
M585646 Miller
c.1 Improved aerosol optical depth and particle size index from satellite detected radiance.